Surface Roughness Measurement using Laser Detection Technique

by

Abdurrahman Saleh Al-Refai

A Thesis Presented to the

FACULTY OF THE COLLEGE OF GRADUATE STUDIES

KING FAHD UNIVERSITY OF PETROLEUM & MINERALS

DHAHRAN, SAUDI ARABIA

In Partial Fulfillment of the
Requirements for the Degree of

MASTER OF SCIENCE

In

MECHANICAL ENGINEERING

March, 1997

SURFACE ROUGHNESS MEASUREMENT USING LASER DETECTION TECHNIQUE

BY

ABDURRAHMAN SALEH AL-REFAI

A Thesis Presented to the

FACULTY OF THE COLLEGE OF GRADUATE STUDIES

KING FAHD UNIVERSITY OF PETROLEUM & MINERALS

DHAHRAN, SAUDI ARABIA

In Partial Fulfillment of the
Requirements for the Degree of

MASTER OF SCIENCE

In

MECHANICAL ENGINEERING

MARCH, 1997

KING FAHD UNIVERSITY OF PETROLEUM AND MINERALS

DHAHRAN, SAUDI ARABIA

This thesis, written by

ABDURRAHMAN SALEH AL-REFAI

under the direction of his thesis committee, and approved by all members, has been presented to and accepted by the Dean, College of Graduate Studies, in partial fulfillment of the requirements for the degree of

MASTER OF SCIENCE IN MECHANICAL ENGINEERING

Thesis Committee :

Chairman (Prof. B. S. Yilbas)

Dr. M. O. Budair
Department Chairman

Member (Dr. S. A. Al-Kaabi)

Dr. Abdallah M. Al-Shehri
Dean, College of Graduate Studies

Member (Dr. Y. N. Al-Nassar)

Date : 8-4-97

كلية الدراسات العليا
COLLEGE OF GRADUATE STUDIES

ACKNOWLEDGMENT

I would like to express and devote my very deep appreciation to those people who contributed to the success of this work. On the head of those contributors is my advisor Professor Bekir Sami Yilbas, I want to thank him for his patience during all this period and for his continuos guidance and support. he made this work interesting and enjoyable, I very much liked working with him. May Allah please him and reward him "Aljannah".

I thank my thesis committee Dr. Yaagoub Al-Nassar and Dr. Saif Al-Kaabi for showing their interest. Also, my very best regards to Dr. M. Budair for facilitating the lab and understanding our problems with an open heart.

My very great appreciation is devoted to Mr. Yonus who is kind, polite and very cooperative. He did not hesitate to work overtime in the central work shop during the design stage, I wish him the very best. Thanks are also devoted to Mr. Coban in the energy lab for helping us in polishing the mirrors.

The effort made by Mr. Abdulhameed in the electrical engineering is quite appreciable. He was available with us for several weeks during the design of the electrical circuits and he provided us with some of the equipment needed in the lab.

Last but not least, I would like to thank Mr. Sayed Fadel in the research institute for his cooperation. He facilitated using the linear profiling instrument to measure the average roughness of all samples.

ABDURRAHMAN SALEH AL-REFAI

CONTENTS

List Of Figures

List of Tables

A B S T R A C T

Name : **Abdurrahman Saleh Al-Refai**

Title : **Surface Roughness Measurement Using Laser Detection Technique**

Major Field : **Mechanical Engineering**

Date of Degree : **March, 1997**

The measurement of surface roughness using the stylus equipment has several disadvantages. A non-contact optical method becomes demanding for measuring the surface roughness of the engineering metals with improved accuracy. One of the candidate for optical method is the use of a laser source in which the reflected laser light intensity from the surface may represent the surface roughness of the illuminated area. Consequently, a relation can be developed between the reflected laser beam intensity and the surface roughness of the metals.

The present study examines the measurement of the surface roughness of the stainless steel samples using a He-Ne laser beam. In the measurement, a Gaussian curve parameter of a Gaussian function approximating the peak of the reflected intensity is measured with a fast response photodetector. To achieve this, an experimental set up is designed. and realized. In the experimental apparatus, fiber-

optic cables are used to collect the reflected beam from the surface. The output of the fiber-optic system is fed to a backpropagation neural network to classify the resulting surface profile and predicts the surface roughness value. The results obtained from the present study is, then, compared with the stylus measurement results. It is found that, the resolution of the surface texture improves considerably in the case of optical method and the neural network developed for this purpose can classify the surface texture according to the control charts developed mathematically.

بسم الله الرحمن الرحيم

خلاصة الرساله

الأســـــــم : عبد الرحمن صالح الصواب

عنوان الرساله : قياس خشونة الأسطح بإستخدام تقنية الليزر

التـخـصـص : الهندسه الميكانيكيه

تاريخ الرساله : شوال ١٤١٧هـ

قياس خشونة الأسطح بإستخدام آلة المرقم له عدة عيوب، من أجل ذلك أصبح وجود آله بصريه لقياس خشونة أسطح المعادن الهندسيه بدون تلامس وبدقه أكبر أمرٌ ضروري . أحد الوسائل المقترحه هو إستعمال مصدر الليزر، حيث أن حدة الشعاع المنعكس من السطح المضاء بشعاع الليزر يمكن أن يعطي معلومات كافيه عن خشونة هذا السطح .

في هذه الأطروحه تم قياس خشونة عدداً من أسطح الفولاذ الصامد بإستخدام الليزر، حيث يسلط الشعاع على السطح ومن ثم يرتد هذا الشعاع وتزيد حدته عندما يكون السطح أملساً وتقل كلما كان أكثر خشونه . حدة الشعاع المنعكس يتم قياسها بواسطة الصمام الثنائي الضوئي، هذا الصمام مزود بوحده لتقوية الإشارات الكهرومغناطيسيه ومن ثم يقوم بربط هذه الإشارات بالحاسوب . يوجد في الحاسوب برنامج تم إعداده، يحتوي على شبكه معلوماتيه من النوع العكسي، هذه الشبكه تقوم بتحليل وتصنيف المعلومات المتعلقه بالسطح ومن ثم إيجاد متوسط خشونة السطح . بعد الحصول على نتائج طريقة الإنعكاس الضوئي ثم مقارنتها بنتائج آلة المرقم ، وجد أن الطريقه الضوئيه أعطت وصفاً دقيقاً لمعالم الأسطح وكذلك وجد أن الشبكه المعلوماتيه صنفت الأسطح بنجاح حسب الأنماط المطوره رياضياً .

درجة الماجستير في العلوم

جامعة الملك فهد للبترول والمعادن

الظهران – المملكه العربيه السعوديه

شوال ١٤١٧هـ

CHAPTER 1

1 - INTRODUCTION :

Surface analysis is one of those technologies that is moving more strongly from the laboratories onto the shop floor because manufacturers are becoming aware of its potential for establishing and proving quality. No part is perfectly round, straight, or smooth, so all have microscopic irregularities. With this information the manufacturer can quantify a surface condition to meet a specification, or track down a problem in the product or the manufacturing process. Several parts failed a quality check at the end of the machining line because, their average surface roughness values (Ra) are neglected by the manufacturing engineer. That was a mistake, since consistent Ra readings can indicate process stability, there's no guarantee that the surfaces produced will function as designed.

In many engineering applications surface texture is closely allied to function, particularly, when the surface concern comes into contact with a moving surface. For example, a surface has to have a certain roughness to hold the oil film used for lubrication as in using lip seals. This type of seal is often interposed between the differential housing and brake mechanism on a motor vehicle rear axle, and if the finish of the shaft is too smooth it will be difficult to maintain a fluid film between the shaft and the seal. On the other hand, if the shaft is too rough it will cause abrasion of the seal and lead to eventual failure.

Many electrical equipment generates heat which could damage , or even destroy a component if the heat is not removed. Conduction of heat from surface to another depends partially on the texture of both surfaces . If the surfaces are rough the contacting area will be small so does the amount of heat removed.

In order to treat defects of the valves and inner walls of the heart, its function is temporarily taken over by a heart-lung machine, the heart can then be opened up and examined. In this condition machine and patient are connected by tubes and it has been found that they can cause damage to the red blood cells. Microscope examination revealed that the bores of the tubes had different roughness. Some definitions may be useful to introduce here. These include surface texture and surface roughness.

Surface Texture :

Surface is defined as the boundary between one material and another. The texture produced by machining covers the whole surface so ideally it should be assessed over an area. Stylus instrument ,however, trace a section profile along a line, not over an area. One may ask how this line can represent the whole area of the surface. Fortunately, most surfaces produced by common manufacturing processes have a texture that is substantially even over a large area.

In addition to the texture imposed on the surface by finishing process, there is an inherent micro-structure due to the crystalline, or even molecular structure of the material. Very few natural surfaces are molecularly smooth such as cleaved mica or topaz, but even these are smooth

to certain limit. The complexity of the surface is the main reason behind proposing many parameters to quantify the surface.

Surface texture consideration begins at the design stage, with the designer specifying, where necessary, the texture required to give a desired performance. This implies that the designer must have the necessary understanding of surface texture and knowledge of how it is measured. The production engineer must then plan the work so that the machine tools used are capable of producing that finish. Since the finish almost entirely the result of the machining process, the machine operator should be aware of what surface texture is. This involves measurement which became so easy, sometimes no more than pressing a button and reading a meter. The users of these instruments often overlook the basis on which the assessment is made, but an understanding of this can lead to more intelligent use of any surface texture instrument.

Design Criteria :

Surfaces produced by various processes exhibit distinct differences in texture. These differences make it possible for honed, lapped, polished, turned, milled, or ground surfaces to be easily identified. As a result of its unique character, the surface texture produced by any given process can be readily compared with other surfaces produced by the same process through the simple means of comparing the average size of its irregularities, using applicable standards and modern measurement methods. It is then possible to predict and control its

performance with considerable certainty by limiting the range of the average size of its characteristic surface irregularities .

Variations in the texture of a critical surface influence its ability to resist wear and fatigue, to assist or destroy effective lubrication, to increase or decrease its friction and / or abrasive action on other parts, and to resist corrosion, as well as affect many other properties that may be critical under certain conditions. Surface texture control should be a normal design consideration under the following conditions :

1 - For those parts whose roughness must be held within closely controlled limits for optimum performance. In such cases, even the process may have to be specified. Automobile engine cylinder walls, which should be finished to about 0.32 μ m and have a circumferential (ground) or an angular (honed) lay, are examples. If too rough, excessive wear occurs, if too smooth, piston rings will not seat properly. Moreover, if lubrication is poor, surfaces will seize or gall.

2 - Some parts, such as anti-friction bearings, cannot be made too smooth for their function. In these cases, the designer must optimize the trade-off between the added costs of production and the market value of the added performance.

3 - There are some parts where surfaces must be made as smooth as possible for optimum performance regardless of cost, such as gages, gage blocks, lenses, and carbon pressure seals.

4 - In some cases, the nature of the most satisfactory finishing process may dictate the surface-texture requirements to attain production efficiency, uniformity, and control. However, the individual performance of the part itself may not be dependent on the quality of the controlled surface.

5 - For parts which the shop, with unjustified pride, has traditionally finished to greater perfection than is necessary, the use of proper surface-texture designations will encourage rougher surfaces on exterior and other surfaces that do not need to be finally finished.

It is the designer's responsibility to decide which surfaces of a given part are critical to its design function and which are not. This decision should be based upon a full knowledge of the part's function as well as of the performance of various surface texture that might be specified. From both a design and an economic stand point, it may be just as unsound to specify too smooth a surface as to make it too rough or to control it at all if not necessary.

Surface Roughness :

Typically, the most commonly used parameter for measuring surface roughness is denoted by Ra, which is *an arithmetical average of the roughness profile*. It is a good general indicator of surface finish, but does not discriminate between peaks and valleys. Surface roughness depends greatly on the processes applied during production phase, Table (1.1) gives typical roughness values for different production processes [19].

Table 1.1 : Typical roughness values obtainable by different finishing processes [19].

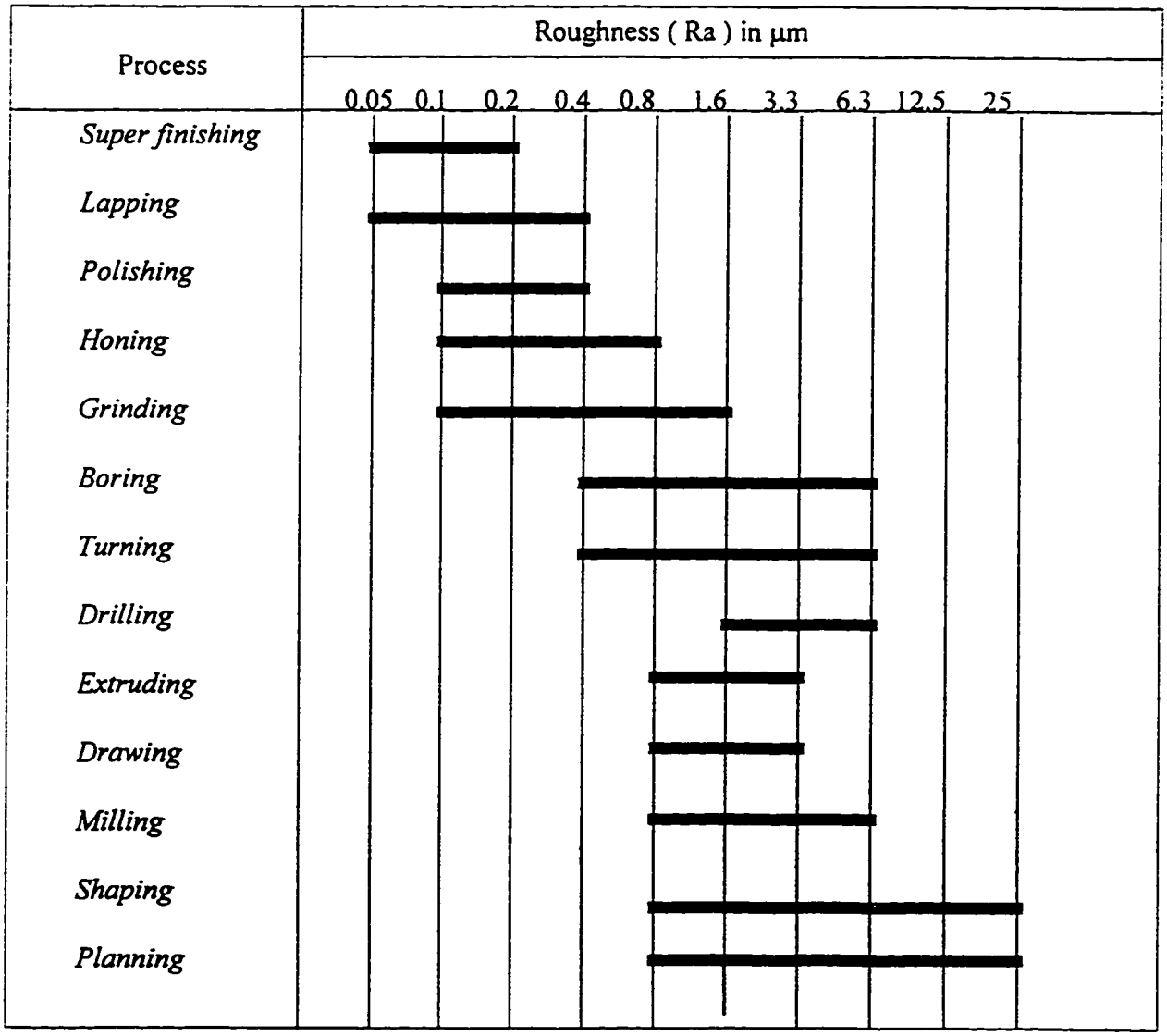

Surface roughness measurements can be obtained using mechanical or optical systems. Nearly 99 % of all surface analyses are done with a stylus-type instrument, this measuring device obtains data much like a needle generates sound from a record [26]. The stylus is drawn over the surface and moves up and down as it follows the surface contours (Fig. 1.1).

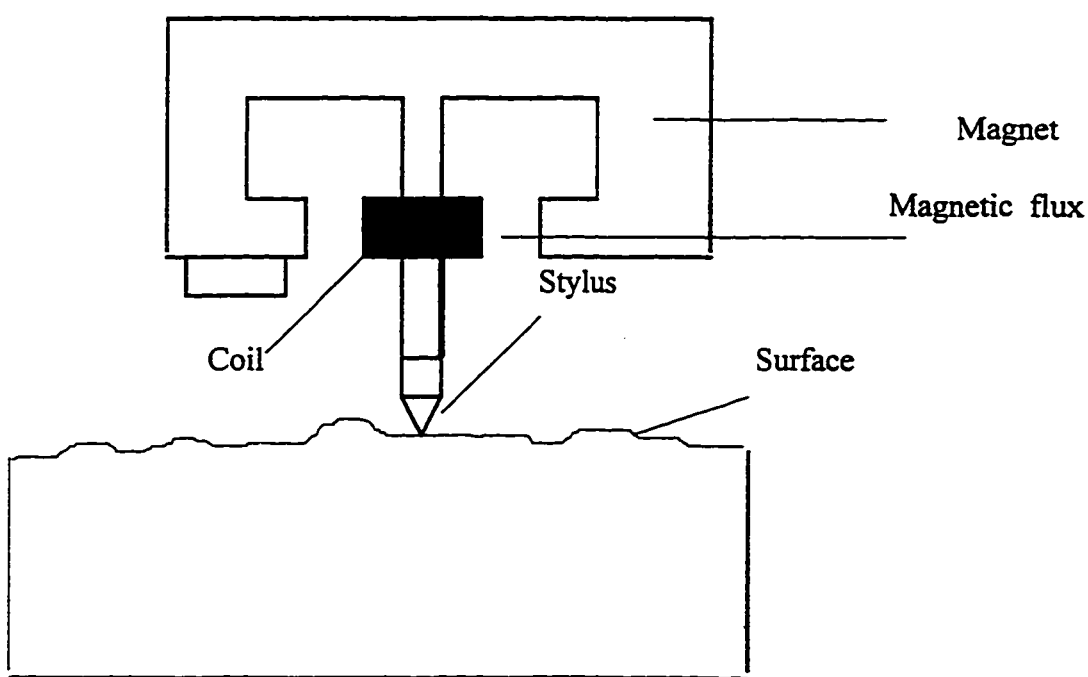

Fig. 1.1 : Moving Coil Pick-up

This motion is sensed by very precise transducers and converted to a surface profile. Most styli are 0.01 mm in diameter with smaller styli used for finer finishes [26]. Vertical travel of the stylus is about 0.13 mm and test paths usually range from 0.4 to 48 mm. There are two types of styli systems : skidded and skidless. Skidded instruments have a skid or foot, the skid limits stylus travel and the stylus holder is pivoted so the instrument can only record roughness parameters. These instruments are more rugged than skidless instrument because the stylus is protected. With skidless instruments the stylus totally free to move up and down, therefore, it can reach more feature with a reasonable accuracy.

1.1 - Literature Survey :

Galante et. al [7] studied surface roughness using a tool image processing technique. By means of tool image detection and processing, the ideal roughness profile that the tool should produce on the workpiece was evaluated. They proposed a model which estimated the value of the effective roughness of the workpiece from one related to the ideal profile which was not influenced by the feed rate employed. The experimental apparatus employed a tool-holder identical to the one on a lathe fiber optic light source, a CCD video camera and a real time video digitizer board installed in a personal computer . To investigate the goodness of the proposed methodology, cutting tests were carried out using CNC lathe with a tungsten carbide tool and working on AISI-1040 steel. The cutting speed was set at 3.33 m / s and the depth of cut was 1 mm with feed range (0.12,0.15 & 0.18 mm). They concluded that, the proposed methodology for the on-line control of the surface roughness in the finishing was able to determine the profile that the tool should ideally produce on the workpiece.

Takashi Matsumura et. al [14] investigated a prediction way of tool wear as well as for surface roughness. It was proposed an autonomous operation planning, which optimized machining operations for each machine tool using adaptive prediction of processes. Machining processes were predicted and optimized more accurately using the adapting parameters of the governing equations of neural networks through learning of

machining results. When considering surface roughness, machining operations were optimized to minimize the cost.

Shukla et. al [24] studied the surface roughness using the interferometric techniques. The proposed techniques were useful in the precise optical alignment of the sample in the Sommargren's profilometer for surface roughness measurements . Using these techniques, the tilt of the sample was eliminated in order to obtain the exact surface profile. They used a-high precision mirror mount which was fixed on a rotary table. The sample could be tilted about two orthogonal axes with an accuracy of about 0.1 arc-second. A parallel plate was chosen as a sample which was coated with aluminum. The bottom surface of the parallel plate was used for measuring its roughness while the top surface was used as the end mirror of the Twyman -Green interferometer. The apparatus of the mirror was chosen to be 25 mm. As an outcome of their measurements, they concluded that interferometric techniques were useful for eliminating the sample tilt for surface roughness measurements. In order to obtain an exact surface profile, the surface tilt had to be eliminated. Also, the interferometric techniques were found to be useful for measuring the wedge angle of the nearly parallel plate made of opaque materials.

Klimezake [27] carried out an experimental investigations of the origins of differences among roughness parameters by considering the surface height distribution of 2 & 3 dimensional characteristics. The sample size and the mean line deviation of profiles from the surface mean plane were found to be responsible for the differences. Investigation of the

magnitude and statistical significance of the differences between some parameters of the 2D and 3D characteristics were carried out on surfaces produced by the common machining processes such as face turning, face milling, grinding and sand blasting. The mapping of the surface texture was realized by means of the stylus technique. He concluded that, the main differences occurring in the surface height distribution estimation in the 2D & 3D approaches were :

(i) the different sample size.

(ii) the fact that the profile's mean lines did not coincide with the surface mean plane.

Parsons et. al [6] discussed the development of a touch screen and related software functions as dedicated keyboard, which presented a very limited number of operational options. Using simple color graphics icons, the described software developed guided the operator through the measurements process via a logical series of questions and menu operations. The program presented only specific questions or options that were relevant to the current measurement which are provided for a more friendly interface between operator and instrument. They concluded that, repeated measurement of identical procedures could be accomplished with a single touch of the screen. These enhancements of the interfaces on surface and roundness gages made them easier for less skilled operator to use.

Myshkin et. al [15] analyzed surface topography using scanning electron microscopy. Scanning electron microscopy could be considered as a powerful instrument for morphology analysis allowing a wide selection of methods for the examination of surface feature. It was shown that it could also be used to measure surface heights at given points. They showed that at identical points due to specimen rotation about coordinate axis depended only on the tilt angle and the profile slope at the section perpendicular to the rotational axis.

Osana et. al [17] pointed out that the problem of workpiece accuracy was of still growing importance in the present time of competition, cost consciousness and computer integrated on the one side and increasing demand for quality and reliability on the other side.

Garratte et. al [11] studied roughness measurement using a stylus instrument, namely Nanostep. The construction of the instrument was mainly of " Zerodur " glass ceramic. The workpiece was mounted on a three-point kinematic support on levelling table, which in turn was mounted on a carriage. The carriage had dry polymeric pads positioned to form an interface with highly polished precision slideway providing a linear traverse of 50 mm. The large barrel micrometer pushed the carriage along the slideway against a salve carriage providing an almost non-influencing drive. The micrometer was driven by a DC motor mounted on a coast iron base, which was isolated from the structure by anti-vibration

mounts. The micrometer was driven at speeds between 0.5 - 0.005 (mm / s). The pick-up assembly was attached to the column and was moved into contact with the workpiece by a micrometer. They concluded that, instrument noise both electrically and mechanically limit the usefulness of an instrument in measuring very fine surfaces. They found that, stylus instrument caused an indentation on the surfaces which contributed to the surface roughness.

A surface roughness measurement was carried out by Kurita et. al [12] using a laser beam source. The optical technique used in the experiment was based on the surface reflection of the grinded surfaces. Aluminum specimens were used where the surface roughness was measured using the Gaussian curve method. A laser beam emitted from a laser generator and then reflected on a mirror, falling perpendicularly to the surface of the specimen and was again reflected. The intensity of the reflected light was measured with plasma coupled device. Linear imaging sensor was inputed into a personal computer. They concluded that, the peak of the reflected light intensity distribution curve could be approximated by a Gaussian function, the Gaussian curve parameter (GCP) calculated from raw data points. Therefore, it was unnecessary to average the intensity data points in evaluating the broadness of the intensity distribution curve by the use of GCP. Also, they found that, GCP increased with increasing surface roughness Ra.

Domanski et. al [5] measured surface roughness utilizing optical fibers. Two methods were used namely : intensity-based and polarization-based. Concerning the intensity-based measurements, a three-branch optical fiber cable with multimode fibers was used in which two branches were coupled to a photodetector. For the polarization-based measurements, a laser light (λ = 633 nm) chopped at 130 Hz was launched along a birefringence axis into a high-birefringence (HB) fiber. This HB fiber preserved the input polarization state of light which was guided to a rough surface. The signal scattered by the rough surface was transmitted through a short length fiber cable which was detected by a photodiode. The distance from the rough surface to the fibers heads was fixed at 0.6 mm. They concluded that, the intensity-based roughness measurement was strongly dependent on distance characteristics which was the essential problem of the method. In the polarization measurement, they measured six intensities for six rough samples and for different positions of input polarization P, the azimuth θ and elepticity ε, the results indicated that there was no correlation between quadratic mean roughness (Rq) and the state of polarization of the light scattered from the sample for various angles α and different configurations. They also concluded that, uncomplicated fiber-optic method with its compact, flexible, remote controllable setup allowed differentiating surface roughness in the range 0f 0.5 - 30.0 μm (Rq) based on either method.

G. Sathyanarayanan et. al [23] utilized a new approach to model the creep feed grinding of super alloys. A back-propagation learning algorithm was adopted to capture the system behavior. The neural network learned to associate the inputs (feed rate, depth of cut, and etc.) with the outputs (surface finish, force, and etc.) and predicted the system outputs within the working conditions. Mathematical formulation of a multiobjective optimization problem was then carried out by utilizing the network models.

Dean Brenner et. al [3] discussed a new application of neural networks to classify signals produced by a dynamic touch sensor, and achieve automated characterization of metal surfaces during machining. Data was first pre-processed and the spectral features were inputted to a feed forward, one hidden layer neural network trained with backpropagation. The classsification accuracy over 90% for most of the surfaces was reported.

Ramamoorthy et. al [2] characterized the textural features form the digitized images using statistical method. Three different machining operations were used namely, grinding, milling , and shaping. Specimens for the experiment were prepared (flat specimens) with various roughness and by controlling the machining parameters, a range of surface roughness values were obtained to analyze the textures. The surface was viewed through a Vadicom Qualifier 866 inspection system with high magnification in order to obtain values of grey level intensity matrix. The pixel intensity values were restricted to the 0-25 range

and the illumination level was at 70. From the grey level histogram, the following observations are made :

(a) There was a shift of the histogram towards higher grey levels as the surface became smoother.

(b) In the case of coarse surfaces, the frequencies of few grey levels were very high.

(c) As the dominance of a few grey levels was observed in the case of coarse textures, it gave a high standard deviation in grey values. Using histograms had the limitation that they carried no information regarding the relative position of the pixel intensities with respect to each other. One way to bring this type of information into texture analysis was to consider the positions of the pixels and this as achieved by the co-occurrence matrices were found to be more sensitive to changes in surface finish than those calculated from the first-order statistics. They concluded that, the textural features were based on statistics which summarize the frequency distribution of the grey values and relative frequency distribution of the grey level values which described how often one grey tone appeared with another grey tone in a specified spatial relationship.

Psang Dian Lin [13] introduced a new generalized methodology to analyze optical elements and systems. The reflection and refraction laws were formulated in the from of a homogeneous transformation matrix. A system to measure the roughness of surface was designed and modeled using this method, and a converging lens was analyzed as an illustrative example. The results showed that the imperfection of this lens could be

easily assessed and the performance of this measurement system was excellent even in measuring surface with orientation changes.

Rzevski et. al [8] divided the neural network into categories based on their structures and training methods and described example in each category. Their paper outlined broad groups of engineering applications of neural networks, cited different applications in the major engineering disciplines and presented some recent applications investigated in the author's laboratory.

Samuel H. Huang et. Al [10] introduced the basic concepts of neural networks and reviewed the current application of neural networks in manufacturing. The problems with the neural networks were discussed and the possible solutions were suggested.

Measurement techniques using optical probes (requiring non-mechanical contacts) was investigated by several researchers. Yilbas et. al [28] studied the development of the computer controlled electro-fiber-optic system for surface roughness measurements and demonstrated that the measurement of the surface roughness could be possible within a limited accuracy. This was due to that they used an ordinary light source which resulted high degree of diffusion of light at various frequencies reflected from the surface. This caused deficiency in reflected beam since photodetector was not sensitive to all the reflected light frequencies.

1.2 - Scope Of The Work :

The use of the mechanical system has several disadvantages and limitations. These may include :

i) On the surfaces with deep valleys, the stylus (measuring probe), because of its tip size, may not be able to penetrate fully to bottom. The larger the tip radius the less will be the measured excursion of the stylus the roughness values, both computed and recorded on the graph, will therefore be smaller.

ii) When a spherical stylus passes over a sharp peak , the point of contact moves across the stylus, from one side to another. This causes the stylus to follow a path that is more rounded than the peak, although because the stylus is raised to its full height when it is directly on the crest, the true peak height may not be measured with any accuracy .

iii) Whenever a re-entrant feature is encountered, the stylus tip loses contact with the profile and, therefore, obliterate this feature on the graph. Surface with re-entrant aspirates exists chiefly in cast iron, sintered and porous materials, and this is one of the reasons why surface roughness measurement on these materials may be misleading.

iv) The surface of the workpiece may be damaged during the mechanical contact between the stylus and the surface. This is very important in the case of mirror finished surfaces.

In the light of the above arguments, the computer control fiber-optic surface roughness measurement system is proposed in the present study. The output of the fiber-optic system is integrated with neural network to classify the pattern developed on the surface detected by the

fiber-optic sensor. This provides useful information about the surface roughness as well as the surface profile variation whether it shows cyclic, increasing, decreasing or normal trends.

The measurement of the surface texture is based on the reflection of incident laser beam from the surface of the workpiece. When the surface of the workpiece conforms scratches, reflected beam intensity fluctuates accordingly, therefore, profile similar to the surface texture of the workpiece can be produced from the reflected beam. The workpiece is placed on a holder which allows it to move in 2-dimensional space. The axial motion parallel to the workpiece surface is precisely controlled using a micrometer with graduation of 0.0254 mm, the micrometer is driven by a stepper motor ,this motor is driven by a computer program. The laser (He-Ne type) beam emitted is directed toward the workpiece surface and the reflected beam from the surface is received by an optical probe. The probe consists of a fiber optic cable and fast response photodiode ,i.e. photodiode is situated at one end of the fiber optic cable.

In order to monitor the variation in the power intensity of the incident He-Ne laser beam, second fiber optic probe is employed. In this case, incident He-Ne laser beam is sampled by about 8 % using the beam splitter, therefore, sampled beam is received by the second fiber optic probe. Consequently, beam reflected from the workpiece surface (Io), received by the first fiber optic probe, is normalized using the sampled beam (reference beam denoted by I). Therefore, variations in the first fiber optic probe output due to intensity fluctuation of the incident beam is eliminated.

The software developed for this particular task provides real time plot of probe response and monitor the position of the workpiece during the measurement. The complete surface profile, Ra (value calculated) and neural network employing back-propagation algorithm are used to test the results and classifying the resulting patterns.

The experiment is repeated for the sets of engineering material surfaces including stainless steel sheets. The results are then compared with the results obtained from the mechanical measurement system (Stylus Apparatus).

CHAPTER 2

SURFACE ROUGHNESS

The present chapter deals with the basic definitions in surface roughness and the formulation of the surface roughness (Ra). These will be given under the following subtitles later in this chapter.

When a part is machined, either a chip or particle of metal is detached by the cutting means or the surface is deformed, leaving in the part a scratch or tool mark which is actually a minute depression or groove. The continuos formation of these grooves by the tool as it passes over the surface results in the finished machined surface. Within each groove the texture is determined by the manner in which the metal is torn or otherwise detached from the solid material; this will apply whether the groove is formed by an abrasive grain of microscopic size or by the wide of a planning machine. If the tool is perfectly guided and chips are uniformly detached all grooves should be of equal depth, the mean level of which forms a flat plane. However, if guiding is not perfect or the cutting is not uniform the grooves can form an undulation surface.

On the other hand, the change from the concept of roughness to that of waviness often depends on the size of the workpiece , i.e. irregularity spacings which would be regarded as roughness on a machine tool spindle might be regarded as waviness. The waviness spacing on large machine components may even be greater than the total over all length of some small workpieces. The

number of waves in the functional length also has some influence on how the irregularities can be classified. It is preferable to separate roughness, waviness and form according to their cause(Fig. 2.1). These can be defined as follows :

i) ***Roughness*** :

The irregularities which are inherent in the production process, left by the actual machining agent (e.g. cutting tool , grit , spark). Roughness is produced only by the method of manufacturing , resulting from the process rather than from the machine. A number of causes can contribute to roughness [15] :

1) The mark left by the tool or grit itself, this will be of a periodic nature for some processes and more random for others.

2) There is the finer structure due to the tearing of the material during machining, the debris of a built-up edge and small irregularities in the shape of the tool tip.

As we have seen, roughness consists of peaks and valleys, when we come to explore the practical significance of peaks and valleys we find that they can have some different functional importance. In some applications peaks have a major effect (i.e. enhancing friction in break drum) but in others, valleys are predominantly of more practical significance (i.e. holding oil film on a surface), in general both peaks and valleys must be considered when measuring roughness. We can change their size by using different feeds and speeds, but we cannot eliminate them. In milling, surface roughness is geometrically related to the tool's nose radius, spindle speed, tool setting, and feed rate [12].

Roughness parameters may fall in three groups : amplitude, spacing, and hybrid. Amplitude parameters reflect variations in profile height and so include roughness average, geometric average, peak-to-valley height, and profile height. On the other hand, spacing parameters are sensitive to variations in the profile's wave length. Hybrid parameters are sensitive to variations in the profile height as well as wavelength.

Roughness is the most important function accomplished among surface parameters since it has a greater effect on performance than any other surface quality. The roughness-height index value is a number which equals the arithmetical average deviation of the minute surface irregularities from a hypothetical perfect surface, expressed in micrometers, μm, if dimensions are in metric, SI units. The term *roughness cutoff*, a characteristic of tracer-point measuring instruments , is used to limit the length of trace within which the asperities of the surface must lie for consideration as roughness. Asperity spacings greater than roughness cutoff are then considered as waviness.

ii) *Waviness* :

That component of the texture upon which roughness is superimposed. It may result from such factors as machine or work deflection, vibrations, chatter and etc. Waviness can be attributed to characteristics of an individual machine; for example, unbalance in the grinding wheel, irregularities in the lead screw used for tool feed, lack of machine rigidity or damping.

Waviness is the more widely spaced component of surface texture. Unlike roughness, waviness is not inherent to the process.

In other words, waviness refers to the secondary irregularities upon which roughness is superimposed, which are of significantly longer wavelength. Waviness can be by a dial indicator or a profile recording instrument from which roughness has been filtered out, it is rated as maximum peak-to-valley distance. For fine waviness control, technique involving contact-area determination in percent (90 , 75 , 50 percent preferred) may be required. Waviness control by interferometric methods is also common.

iii) ***Form*** :

The general shape of surface, neglecting variations due to roughness and waviness can be called as form. Noting that, it is usual to mention of "form error" , which is the departure from the intended shape of the surface, caused generally by insufficient rigidity in the means used to support the workpiece, allowing it to bend or deflect under the machining forces; a slideway used to guide the cutting head or workpiece can also cause form errors if it is not straight. Strain in the material, due possibly to heat treatment may cause a surface to bow. Form errors due to these causes can normally encompass only a few undulations (often only one within the length of surface being assessed).

Roughness, waviness and form are three ways in which a surface can depart from perfect smoothness flatness; although always found in combination, the effects on performance are different and by choosing the appropriate sampling length, can often be separately assessed. Roughness and waviness constitute the texture of the surface.

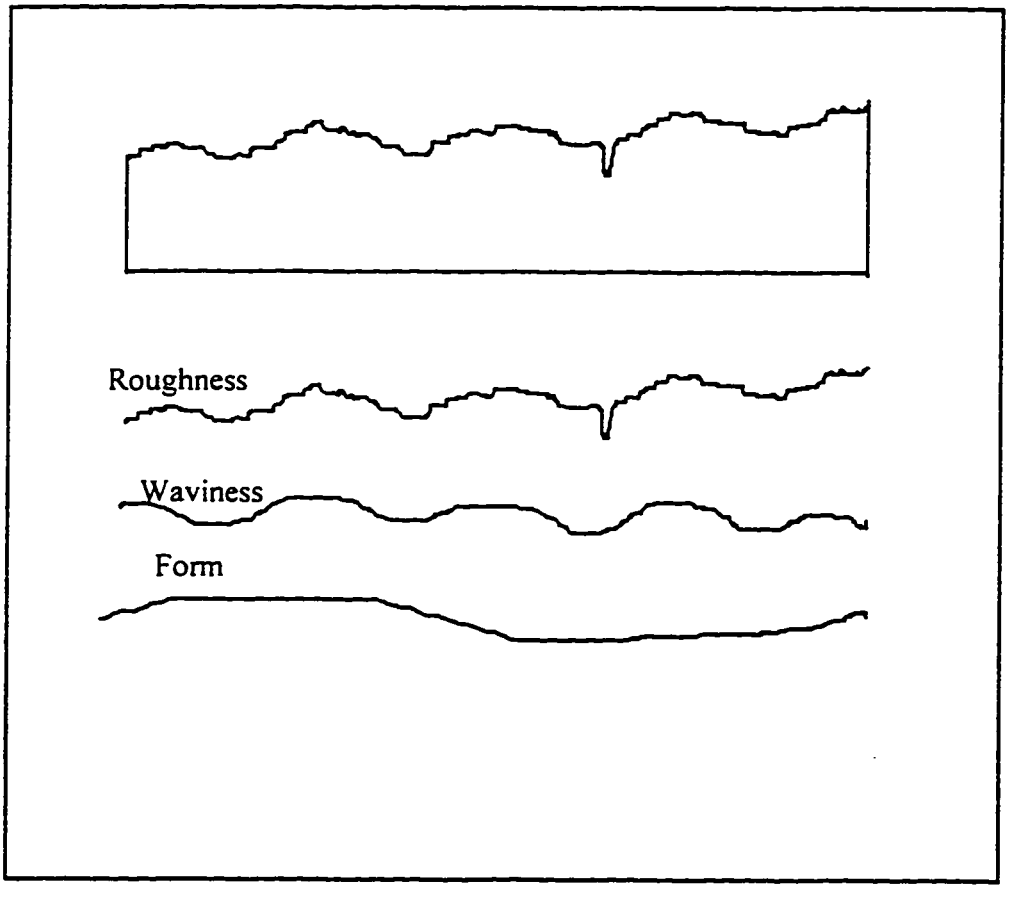

Fig. 2.1 : A surface profile represents the combined effects of roughness , waviness and form .

The derivation of roughness average (Ra) can be graphically illustrated as shown in Figure (2.2), providing that the international surface texture measuring system is employed [22]. The portions of the profile below the center line within the sampling length "L" are inverted and placed above the center line; Ra is then the mean height of the resulting profile.

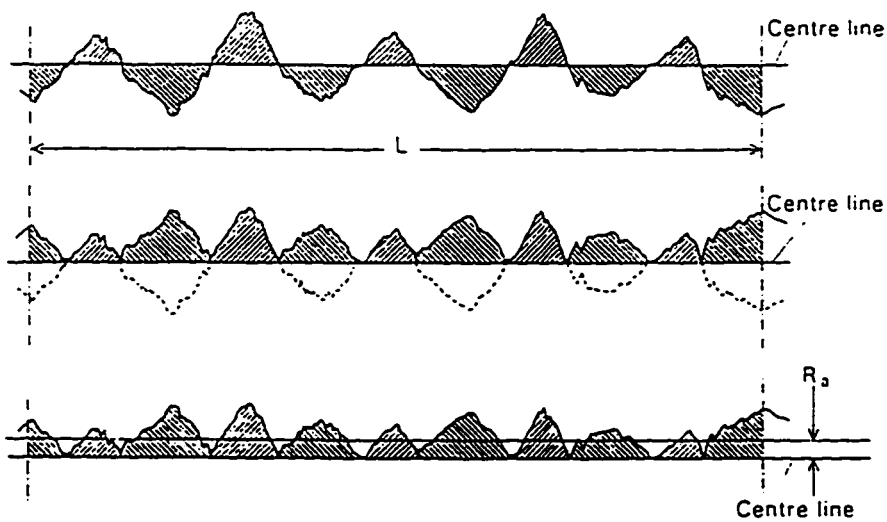

Fig. 2.2 : Graphical Derivation of Ra.

Mathematically Ra is the arithmetic average value of the departure of the profile from the center line throughout the sampling length, the Ra value may be written as :

$$Ra = \sum_{n=1}^{n} 1 / Le \int_{x=0}^{x=Le} Zi \, dx \qquad (2\text{-}1)$$

Where Le ,n and Zi are the sampling length, number of sampling and maximum peak to valley height within the sampling length respectively.

In order to make Ra dimensionless, the below argument can be carried out;

$$\overline{R}a = \frac{Ra}{Zi / m} \qquad (2\text{-}2)$$

Where $\overline{R}a$ and m are the dimensionless roughness average and the number of maximum peak to valley height occurring within the total sampling length. The $\overline{R}a$ value may be related to roughness grades.

Since the *Ra* of a surface can vary quite considerably without significantly affecting performance, it is usual to specify on drawing not the optimum design texture, but a tolerance band within which the texture is acceptable, or even just the maximum roughness that is permissible. Based on this practice, these tolerance bands or roughness grades as they are called, have been given a number distinguished by the prefix N, as set out in Fig. (2.3). The higher the number the rougher the surface. Note that each consecutive number represents a doubling of the *Ra* value, i.e. the grades are allocated in geometrical progression, which accords well with performance.

The grades represent the *maximum* roughness because in most applications it does not matter, from a performance aspect, if within limits, the surface is smoother than that specified. For example, a finish of 0.6 μm *Ra* will satisfy the requirement for a grade N6 or N9 surface, but not for one of grade N5. The use of grade symbols prevents any ambiguity as to whether an *Ra* value is quoted in μm or μin.

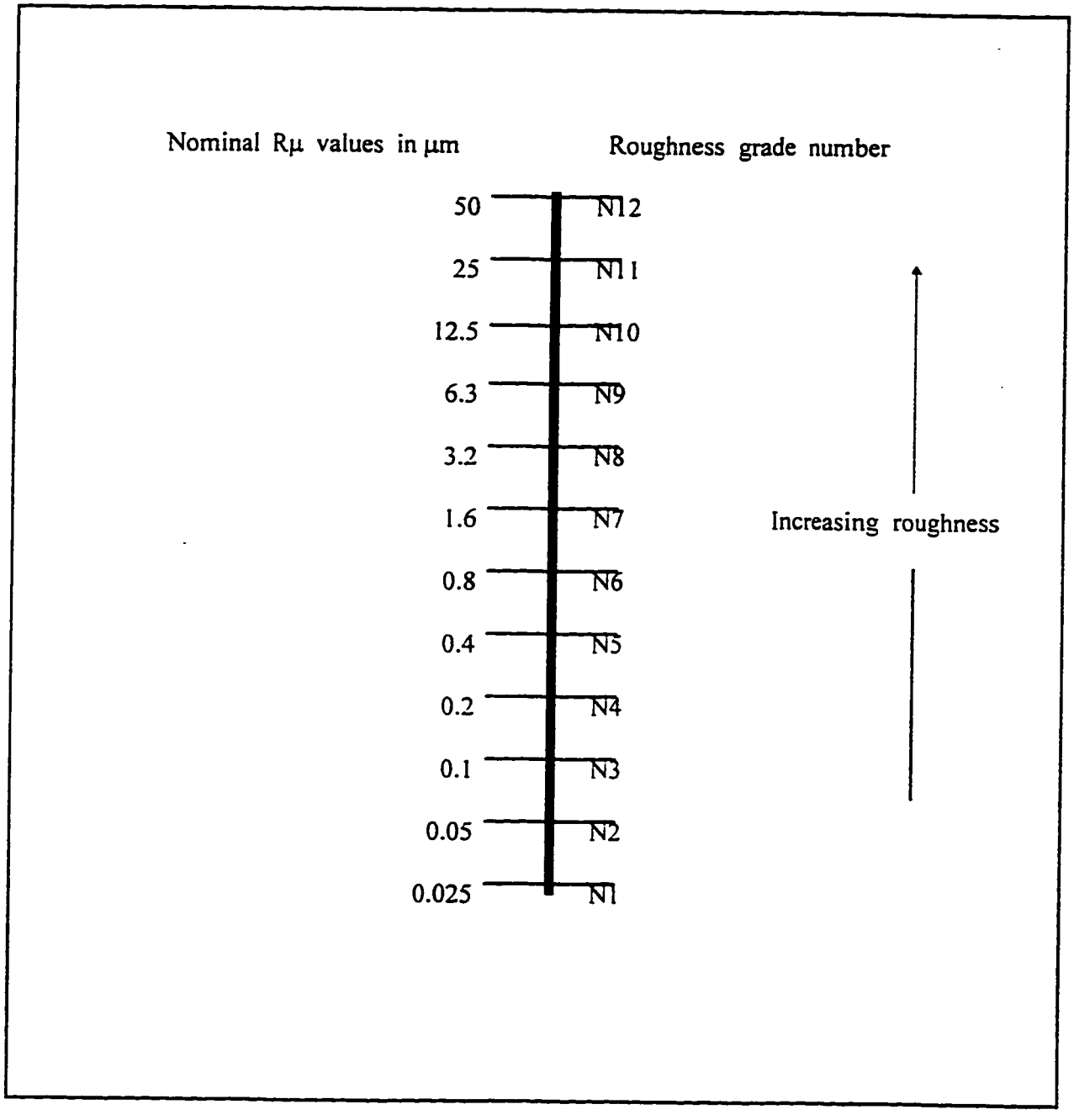

Fig. 2.3 : Roughness grades [19].

The machining pattern on many surfaces has a distinctly directional characteristics called the *lay*, which can be classified into seven main types namely : Parallel, Perpendicular, Crossed, Multi-directional, Particulate, Circular and Radial. These surfaces produce different profile graphs (Fig. 2.4) and have different measured values according to the direction in which the stylus traces the surface.

Lay direction is important in surface texture measurement and the trace should be made across the lay. For machining processes which generate straight, circular or radial lays, the direction in which to make the measurement is usually obvious by visual inspection (with a magnifying glass if necessary). Crossed lay is usually traced at 45° , thus averaging the effect of the two directions.

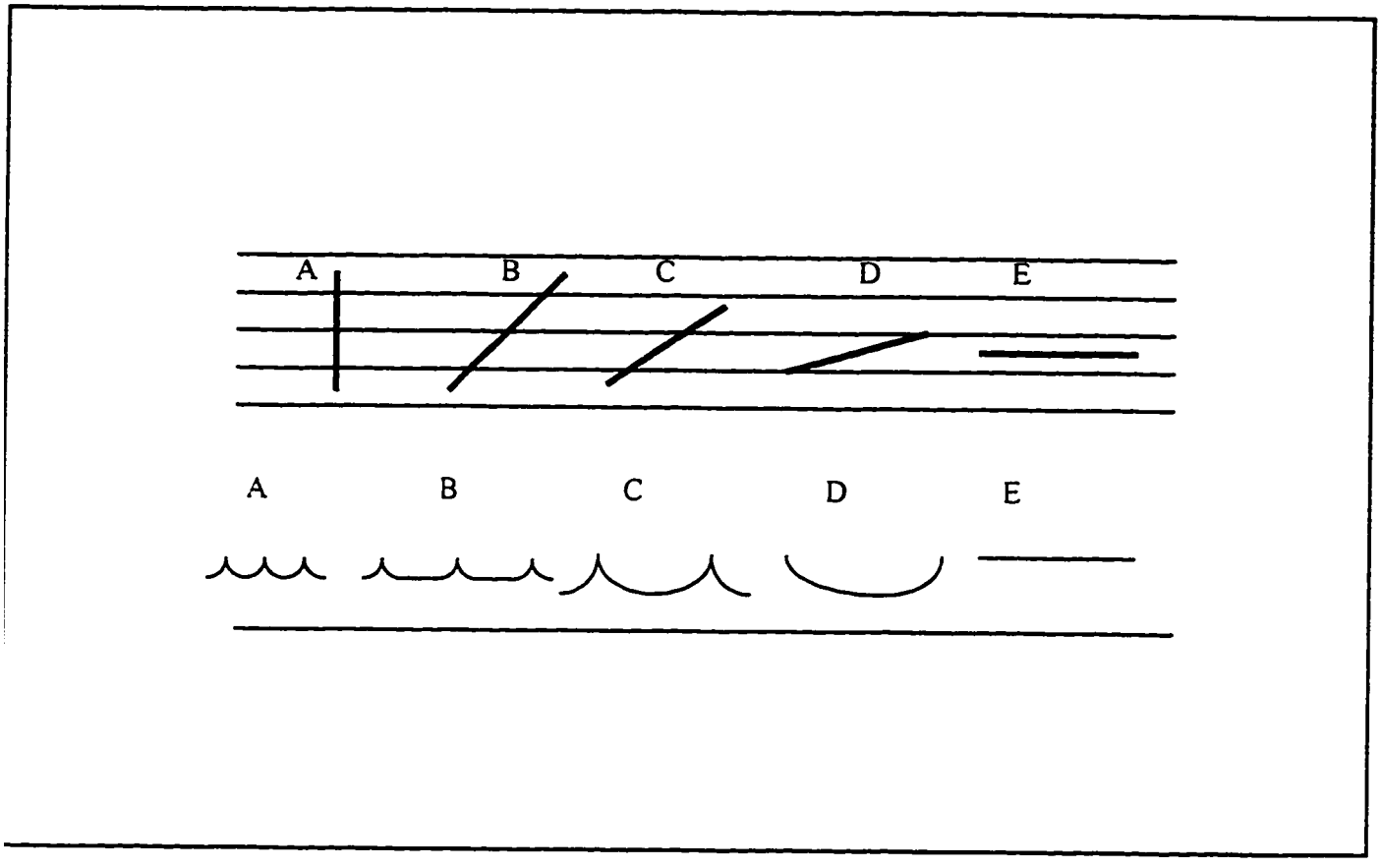

Fig. 2.4 : Effect of relative direction of lay and measurement on profile shape .

CHAPTER 3

SURFACE ROUGHNESS MEASUREMENT

3.1- Technique and set up :

The surface roughness measurement technique relies on the reflection of a laser beam from the engineering surfaces. It is this reflection detected and analyzed to determine the RMS value of the surface roughness. The geometric configuration of the fiber-optic probe and its position relative to surface is very important. The fiber-probes carrying incident laser light is initially set 45° angle to the surface. Consequently, both probes are positioned as perpendicular to each other. However, this probe setting may not be suitable to receive enough light intensity to be detected by the photodiode, therefore, the intensity of He-Ne laser output power is regulated using a beam attenuater. To study the effect of probe position on the measurement accuracy, probe setting is altered in radially , i.e. it is first set to 45° angle to normal direction then decreased to give a probe angle of 10°.

To obtain high precession in determining the probe angle, adjustable mirror holder is used. Gold plated mirror is mounted onto the holder. The probe response (photodetector output) is obtained for a different holder position while changing the probe angle. Therefore, the angle maximizing the probe output is determined. It should be noted that gold plating was carried out using spitting instrument, i.e. about 2×10^{-8} m coating thickness was achieved.

The distance between the fiber-cable probe end and workpiece surface is varied to obtain maximum probe response (detector output). Once the probe response is maximized it is set to this length.

3.2- Equipment :

The mechanical design relevant to experimental setup consists of 10 units. The experimental setup is shown in Figure (3.1), the units include :

1- *Reference Probe & Laser Holder* : This part is designed mainly to support the laser source cable (including prismatic lens) and the reference detector probe (see appendix, Fig. A.1).

2- *Attached Arc (movable)* : This arc is fastened by screws and moves about the main arc carrying the micrometer and the fiber probe (see appendix, Fig. A.2).

3- *Sample Holder* : This unit is made of steel and designed to hold the sample as it being scanned. It's motion is precisely governed by a micrometer.

4- *Main Arc (stationary)* : It has an external radius of curvature of 112 mm and a total angle of 120°. It enables to adjust both the incident laser beam and fiber-optic probe at appropriate positions (see appendix, Fig. A.3).

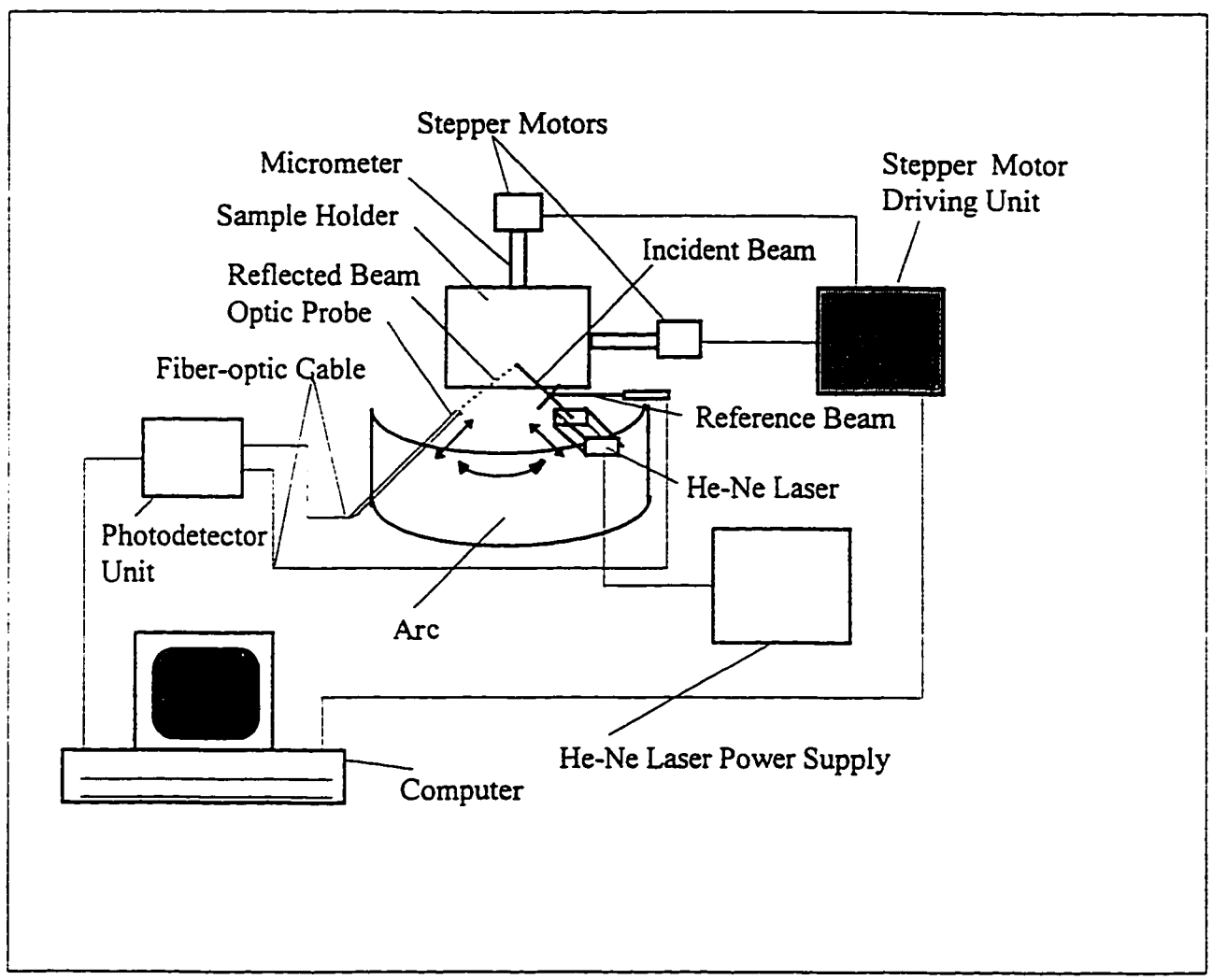

Fig. 3.1 : Experimental Apparatus .

5 - *Main Plate* : Supporting the whole design, it has dimensions of 280 mm length, 150 mm width, and 20 mm in thickness. It rests on four adjustable screws to insure the stability of the design (see appendix, Fig. A.4). A compound cross sectional view is shown in Fig. A.5.

6- *Threaded Screws* : Two of them are installed to allow the movement of laser source and the fiber-optic probe.

7- *Micrometer* : Two identical micrometers have been installed, they have a precession range of 0.001". They are provided with non-rotating spindle with ratchet stop and lock nut.

8- *Threaded Fasteners* : Four of them are mounted.

9- *Washers* : Two pieces are used to prevent any tilt of the holder.

10- *Test Specimen* : Five samples of stainless steel have been prepared, they are polished differently (they have a length of 70 mm and a width of 50 mm).

11- *Adjusting Screws* : Four screws are fixed at the bottom of the main plate to secure the whole design from vibration and instability.

Electrical parts in this experiment consist of the following :

1- *Stepper Motor* : 1.8° stepper motor type is used, it has a holding torque of 460 mNm and a weight of 600 g. The motor is driven by a computer program, it allows the workpiece to be scanned by laser beam until the required length is achieved. The stepper motor with 4-phase construction results higher working torque and stepping rates than those available from the permanent magnet types. It maintains very high resolution due to the small step angle. Applying the correct electrical pulse results in a 1.8° step angle rotation of the spindle (i.e. 200 steps / revolution). When correctly loaded and driven these motors will produce discrete output steps. The number of steps and speed of rotation are respectively determined by the number of pulses and frequency of the input signal. This provides an ideal method of both speed and position control.

2 - *Stepper Motor Drive Board :* A uni-polar drive board (see appendix Fig. A.6) is connected to the motor which is capable of driving any 4-phase stepper motor up to 2A , 30 V dc / phase. The board may be used as a stand alone unit in conjunction with external logic. The board has some features among these are :

- 4 - phase unipolar motor drive up to 2 A / 30 V d.c per phase.
- Full step and half step drive modes (for higher resolution, greater performance stability and faster stepping rates).

- On-board 12 V , 50 mA d.c. output for external use.
- Drive board and the motor can share the same d .c. power supply.

3 - *Amplifying Unit* : Two amplifying units have been used; one for the incident laser beam and the other for the reflected laser beam from the specimen. The laser light is carried out to the amplifying circuit through a fiber-optic probe (has 0.50mm core diameter and gives attenuation of the order of 1000 dB/km), at the end of the fiber optic cable there is a photodiode. Each photodiode is connected to a chip of an INA101 HP type, the chip is highly accurate, multistage integrated-circuit instrumentation amplifier, designed for signal conditioning where high performance is required. The amplifying circuit is connected to A/D converter (427 E) which is interfaced with the computer by a standard PIO card.

4 - *Photodiode* : Two photodiodes were used; one for the reflected laser beam and the other for the reference fiber cable. These photodiodes are very sensitive to light because of the sensing element installed inside them. The maximum forward current is 100 mA. The maximum dissipation of heat is 200 mW at room temperature (25 °C). They have a capacitance of 12 μF and a response time of 250 ns.

5 - *Laser Source* : A high quality 1 mw visible laser (He-Ne)diode module consisting of a laser diode, with a wavelength of 670 nm. The adjustable lens provides a highly collimated beam making it ideal for precession applications such as alignment, edge detection and targeting. The spot size can be easily adjusted using the focusing tool provided. The laser can be amplitude modulated using digital or analogous signals over a frequency range of 100 kHz to 50 MHz making it ideal for data transmission.

6 - *Analog-to-Digital (A / D) Converter* : The *A / D* conversion is a quantizing process whereby an analog signal is represented by equivalent binary states; this is opposite to the *D / A* conversion process. Analog-to-Digital converters can be classified into two general groups based on the conversion technique. One technique involves comparing a given analog signal with the internally generated equivalent signals. The second technique involves changing an analog signal into time or frequency and comparing these new parameters against known values. The successive approximation and the flash types are faster, but generally less accurate than the integrator and the voltage-to-frequency type converters. Furthermore, the flash type is expensive and difficult to design for high accuracy.

3.3- Flow Diagram :

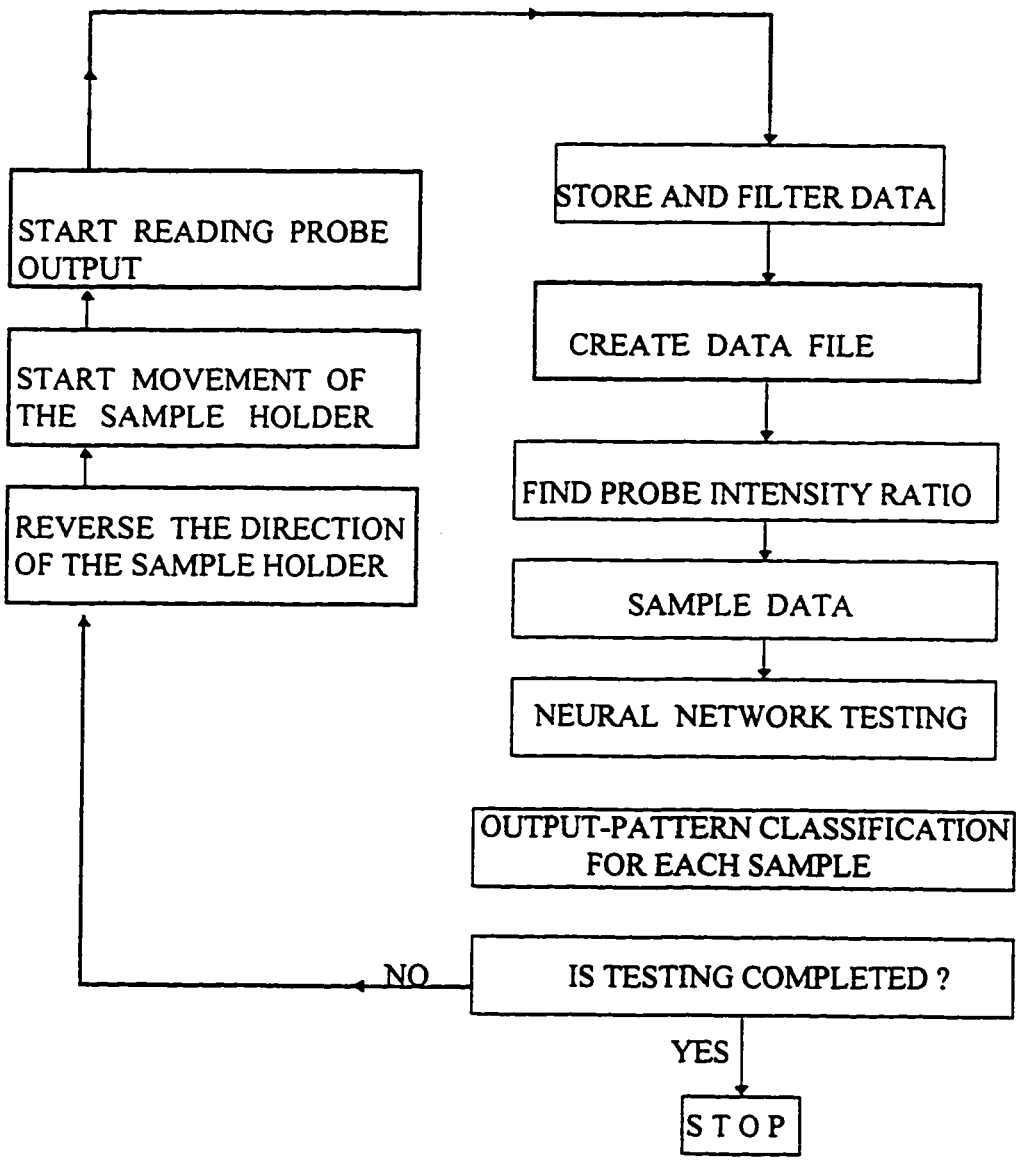

Fig. 3.2 : Flow Chart Showing Surface Roughness Measurement Mechanism.

CHAPTER 4

NEURAL NETWORKS

4-1: INTRODUCTION

Neural networks can roughly be characterized by three classes of features : their architecture or connectivity, their performance or operating rules, and their learning rules. Artificial neural networks developed over the past decade exhibit a range of features along these three dimensions, allowing them to be roughly group according to three architectural features. (number of layers, feed-forward only or feedback connectivity unidirectional versus bidirectional connections), two learning features (correlation or " Hebbian" rules versus error connectivity rules, supervised versus unsupervised training), and one performance dimension (static versus dynamic performance). Although many subdivisions are possible and, in the limit, each neural network could be placed as a single member of its own category, the above dimensions provide fairly good covering of the existing realm of the techniques used in artificial neural networks as described in the literature. Novel networks variants exhibit distinct computational behavior, and much remains to be learned about the value of the various attributes of such networks in terms of their contribution to particular critical operation features, such as learning speed, generalization, capacity and error rate. The present report includes the terminology related to neural networks, rules governing the learning mechanisms, basic operations and architectures of the neural networks.

4 - 2 : BACK - PROPAGATION ALGORITHM :

Back-propagation is the most widely used of the neural network paradigms and has been applied successfully in applications studies in a broad range of areas. Applications studies have spanned tasks from military pattern recognition to medical diagnosis, and from speech recognition and synthesis to robot and autonomous vehicle control. Back-propagation has been applied to character recognition, sonar target recognition, image classification, signal encoding, knowledge processing, and a variety of other pattern-analysis problems. Back-propagation can attack any problem that requires pattern mapping. Given an input pattern, the network produces an associated output pattern.

Back-propagation learning with update procedure is intuitively appealing because it is based on a relatively simple concept : If the network gives the wrong answer, then the weights are corrected so that the error is lessened and as a result future responses of the network are more likely to be correct.

Back-propagation networks are usually layered. Each layer is fully connected to the layers below and above. When the network is given an input, the updating of activation values propagates forward from the input layer of processing units, through each internal layer to the output layer of the processing units. The output units then provide the network's response. When the network corrects its internal parameters, the correction mechanism starts with the output units and propagates backward through each internal layer to the input layer, hence the term back-propagation. Back-propagation is a tremendous step forward compared to its predecessor, the perceptron. The perceptron was limited to only two layers of processing units, with only a single layer of adaptable weights. This key limitation meant that the perceptron could only classify patterns that were linearly separable. Back-propagation overcomes this limitation because it can adapt two or more layers of weights, and uses a more sophisticated learning rule. The power of back-propagation lies in its ability to train hidden layers and thereby escape the restricted capabilities of single-layer networks. Each middle - or hidden - layer acts as a layer of " feature detectors " units that responds to specific features in the input pattern.

An Overview :

Typically, back-propagation employs three or more layers of processing units. Figure (4.1) shows the topology for a typical three-layer back-propagation network. The bottom layer of units is the input layer - the only units in the network that receive external input. The layer above is the hidden layer, in which the processing units are interconnected to layers above and below. The top layer is the output layer.

The layers in Figure (4.1) are fully interconnected - each processing unit is connected to every unit in the layer above and in the layer below. Units are not connected to other units in the same layer. A back-propagation network must have at least two layers. A back-propagation neural network is trained by supervised learning. The network is presented with pairs of patterns - an input pattern paired with a target output. Upon each presentation, weights are adjusted to decrease the difference between the network's output and the target output. After training is stopped, the performance of the network is tested.

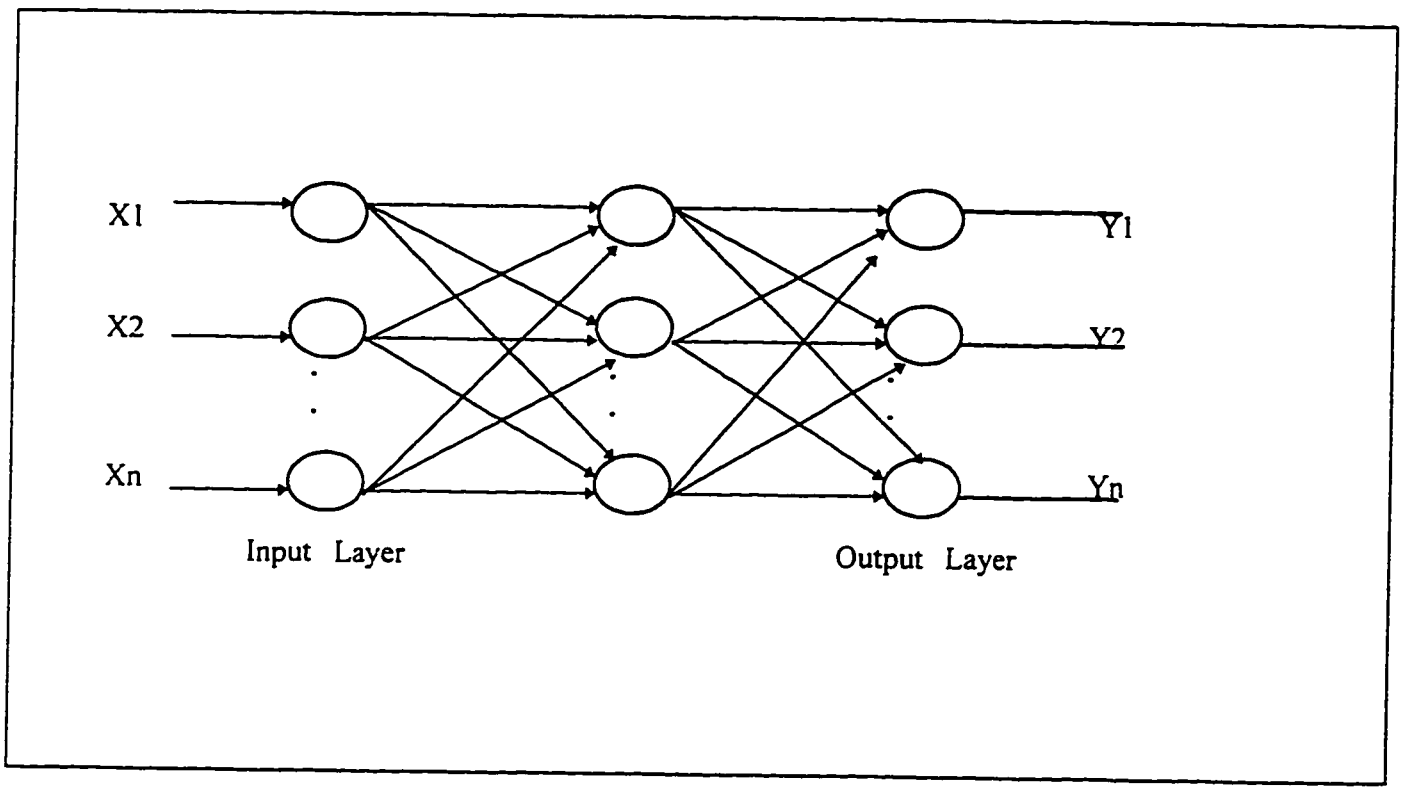

Fig. 4.1 : A counter - propagation network .

Mathematical Formulation :

The back-propagation learning algorithm involves a forward-propagating step followed by a back-propagation step (as explained below). Both the forward and the back-propagation steps are done for each pattern presentation during training [15]. The forward-propagation step begins with the presentation of an input pattern to the input layer of the network, and continues as activation level calculations propagate forward through the hidden layers. In each successive layer, every processing unit sums its inputs and then applies a sigmoid function to compute its output. The output layer of units then produces the output of the network. Output values from input units are summed by :

$$S_j = \sum_i a_i w_{ji} \qquad (4-1)$$

where a_i = the activation level of unit i , and w_{ji} = the weight from unit j (unit i is one layer below unit j). After the incoming sum is computed, a function f is used to compute $f(S_j)$ which is the sigmoid function (Figure 4.2). The sigmoid function is given as :

$$f(S_j) = 1 / (1 + e^{-sj}) \qquad (4-2)$$

after the sigmoid function is evaluated, the resulting value becomes the activation level of unit j. At the output layer calculations start and progress backward through the network to the input layer. The error correction step takes place after a pattern is presented at the input layer and the forward propagation step is complete. Each processing unit in the output layer produces a single real number for its output, which is compared to the target output specified in the training set. Based on this difference, an error value is calculated for each unit in the output layer. Then the weights are adjusted for all of the interconnections that go into the output layer. Next an error value is calculated for all of the units in the hidden layer that is just below the output layer. Then the weights are adjusted for all interconnections that go into the hidden layer. The error value denoted by the variable δ_j is computed as :

$$\delta_j = (t_j - a_j) \quad f'(S_j) \qquad (4-3)$$

where t_j = the target value for unit j

a_j = the output value for unit j

$f'(S_j)$ = the derivative of the sigmoid function (Figure 4.2)

S_j = weighted sum of inputs to j

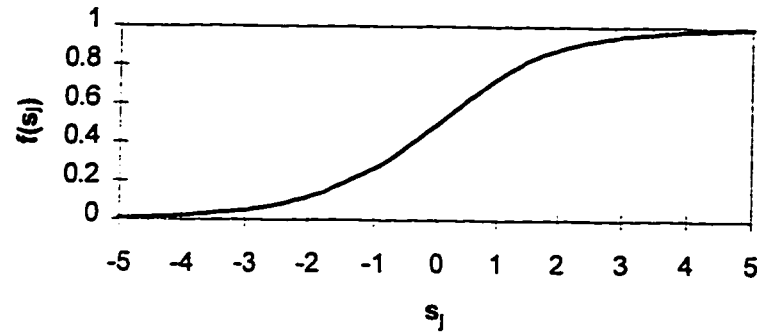

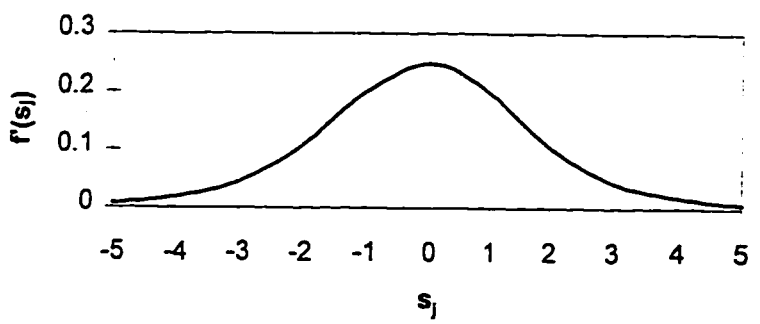

Fig. 4.2 : The sigmoid function (up) compared to its derivative (below)

The quantity $(t_j - a_j)$ reflects the amount of error. The f' part of the term " scales " the error to force a stronger correction when the sum S_j is near the rapid rise in the sigmoid curve. When unit j is in the hidden layer, the error is as :

$$\delta_j = [\ \Sigma w_{kj}\ \delta_k\ ]\ f'(s_j) \qquad (4-4)$$

The connection weight adjustment is done as follows :

$$\Delta w_{ji} = \eta\ \delta_j a_i \qquad (4-5)$$

This weight adjustment equation is known as the generalized δ rule [21] ; the amount adjusted depends on three factors : η , δ_j and a_i . The variable η in the weight adjustment equation is the *learning rate*. Its value is commonly between 0.25 and 0.75 is chosen by the neural network user.

Network Training :

Back-propagation networks are trained by a technique called *supervised learning*, whereby the network is presented with a series of pattern pairs, each pair consisting of an input pattern and a target output pattern. Each pattern is a vector of real numbers. The target output pattern is the *desired* response to the input pattern and is used to determine the error values in the network when the weights are adjusted.

The target output pattern is sometimes designed to represent a classification for the input pattern. In this way, the network may be presented with a series of input patterns together with the classification for each input pattern. In other applications, the target output is simply a desired pattern response to the input pattern, and the network is trained to be a pattern-mapping system.

Convergence :

When a network is trained successfully, it produces correct answers more and more often as the training session progresses. It is important, then, to have a quantitative measure of learning. The root-mean-squared (RMS) error is usually calculated to reflect the degree to which learning has taken place in the network.

This measure reflects how close the network is to getting the correct answers. As the network learns, its RMS error decreases. Generally, an RMS value below 0.1 indicates that a network has learned its training set, it can be computed by the equation :

$$RMS = \left(\left(\sum_p \sum_j (t_{jp} - x_{jp})^2 \right) / (n_p n_o) \right) 1/2 \qquad (4-6)$$

where n_p = number of patterns in the training set

n_o = number of units in the output layer

t_{jp} = the target value for output unit j after presentation of pattern p

x_{jp} = the output value produced by output unit j after presentation of pattern p

Whether an answer is correct or not is a binary Yes / No decision. The target value to a network is a real number, and so is the output value. Thus , the network does not provide a Yes / No response that is either " correct " or " incorrect " . The network gets closer and closer to the target value incrementally with each step. It is possible then to define a cutoff point when the network's output is said to match the target values, and allow this to define a " correct " answer. Convergence is a process whereby the RMS value for the network gets closer and closer to 0. Convergence is not always easy to

achieve because the process may take an exceedingly long time and sometimes the network gets stuck in a local minimum and stops learning altogether.

Network Testing And Performance :

Typically an application requires both a training set and a test set. Both the training set and the test set contain input / output pattern pairs. While the training set is used to train the network, the test set is used to assess the performance of the network after the training is complete.

The principle strength of back-propagation algorithm is its relatively general pattern mapping capabilities; it can learn a tremendous variety of pattern-mapping relationships. Back-propagation merely needs examples of the mapping to be learned. The flexibility of the paradigm is enhanced by the large number of design choices available : number of layers , interconnections, processing units, the learning constant, and data representations. As a result, back-propagation algorithm might be able to address a broad spectrum of applications.

4 - 3 : NEURAL NETWORK USED IN THE SYSTEM

To develop input vectors for the neural network, the data file obtained from the optical measurement for each workpiece surface is divided into 10 sub-data files providing that each sub-data file contains 100 of data points. Consequently, the number of neurons in the input layer is fixed as 100. In the second step, the type of output used should be decided. Consequently, 4 digit binary vector is used as output relevant to the number of workpiece surfaces, i.e. four processing elements take part in the output layer of the back-propagation network. The process of determining the number of hidden layer elements has been carried out on trial and error basis . If the number of processing elements is high in the hidden layer, the network will lose its ability to generalize; and if a few number of processing elements in the hidden layer, the network can not be able to learn. As a result of this, it is found that 53 processing elements in the hidden layer gives improved performance. Each connection weight is initialized to a small random number. A data file is developed mathematically to train the network. The network is, then, trained and being tested to recognize the input vectors under noisy or uncertain conditions.

A computer program for a back-propagation neural network has been developed to recognize the input vectors relevant to each surface and interpret the output of the network. Consequently, the network developed has 100-53-4 neurons structure in input-hidden-output layers as shown in figure (4.3).

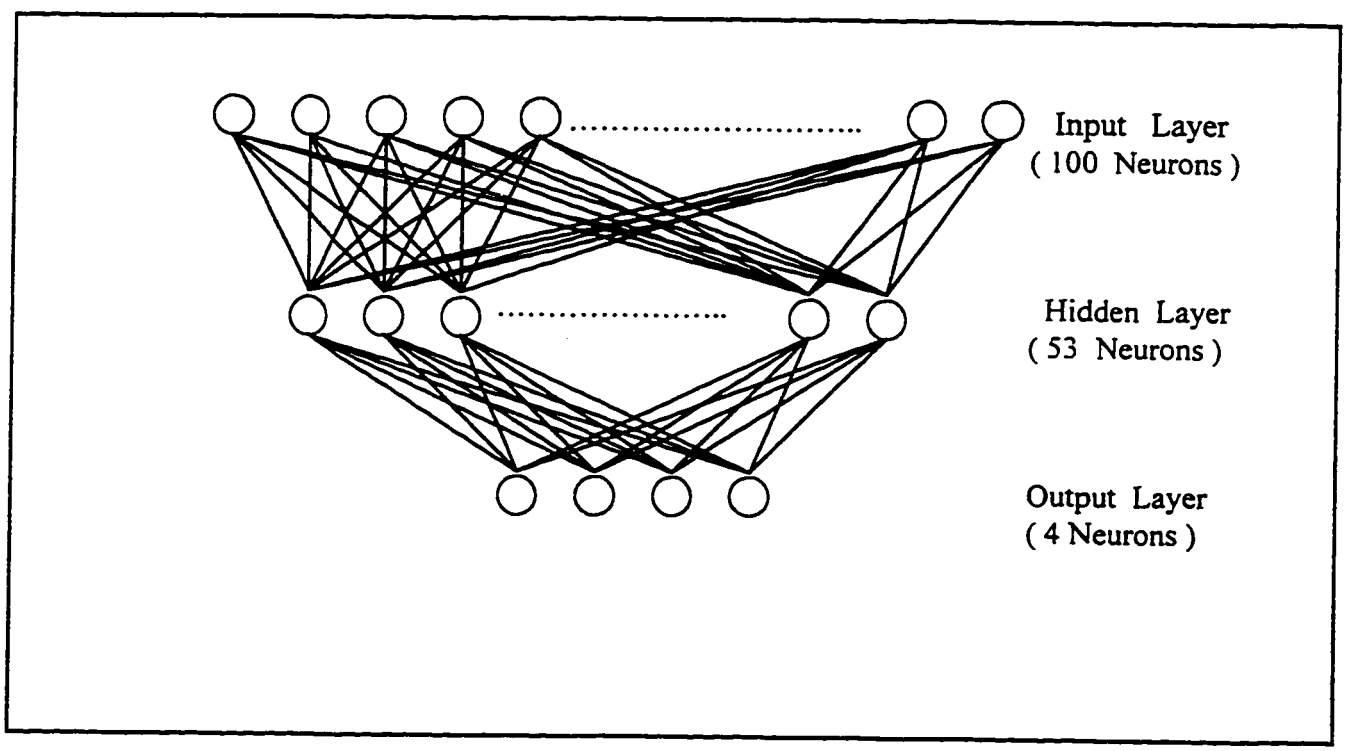

Fig. 4.3 : Schematic view of back-propagation net work.

The performance of the network can be defined as :

$$\text{Performance} = \frac{\text{Number of Patterns Correctly Classified}}{\text{Number of Tests for the Pattern}}$$

Therefore, all the data obtained from the optical method is tested and performance analysis are obtained.

CHAPTER 5

RESULTS AND DISCUSSIONS

5 - 1 : PROBE POSITION ANALYSES :

The gold coated mirror was used to calibrate the probe response relative to the probe position. During the calibration of the probe, the first probe position was set at 9 mm from the workpiece surface and this distance was increased gradually 1 mm at a step using a micrometer. The maximum displacement of the probe from the initial point was 23 mm. It should be noted that the selection of the initial probe position during the calibration was based on the probe response. In this case, a distance closer to the surface (less than the initial probe position) did not affect the probe response, i.e. in the range of 9 mm from the surface to the initial probe setting, the probe response is all the same . Therefore, discussions relevant to the probe calibration is given below :

The variation of the probe response with distance (probe position to workpiece surface) is shown in Figure (5.1) for the case of sample holder parallel to the workpiece. The probe response is almost constant up to the distance

of 10 mm away from the workpiece surface, once this distance is increased further, the probe response drops rapidly and decays. This may be due to the fact that, the reflected beam has enough power intensity to be detected by the probe. However, as the distance is increased considerably, the intensity reduces due to divergence of the reflected beam. When examining the case at which the attenuater is situated in the path of incident beam, the probe response does not change considerably from the no-attenuater case. This indicates that, the effect of the beam attenuation is negligible on the probe response. On the other hand, some fluctuations are evident in the probe response, especially, when the probe is close to the workpiece surface. This may be due to the noise in the detection system as well as interference due to existing environmental lights.

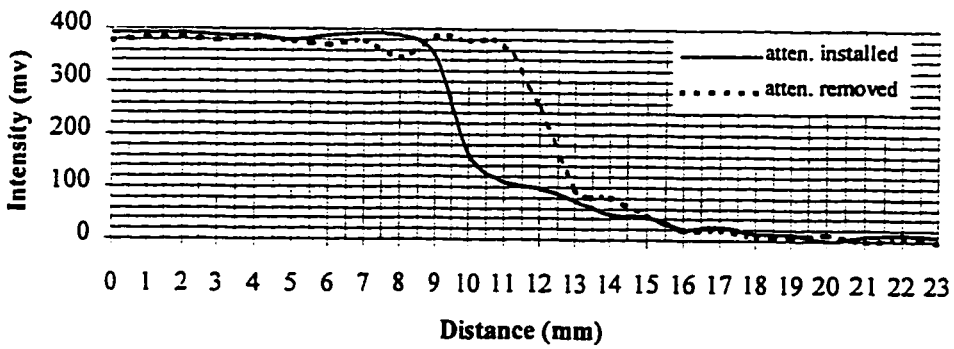

Fig. 5.1 : Intensity Variations (sample parallel to holder)

In the second case where the sample holder is inclined with a positive 5° angle, the probe response is almost constant up to a distance of 8 mm as shown in Figure (5.2). After the distance of 8 mm the intensity drops sharply within a distance of 3 mm and then, decays. As might be depicted from the figure, the sudden drop in the intensity occurs at earlier stage than for the first case (parallel). This may be due to the divergence occurred to the beam after tilting the sample with an angle of + 5 °. Near the workpiece, some reflected beam intensity fluctuations take place. This may be due to noise (environment + system), occurring during the measurement. The attenuater does not have a notable effect on the intensity profile since the two curves overlap each other most of the times.

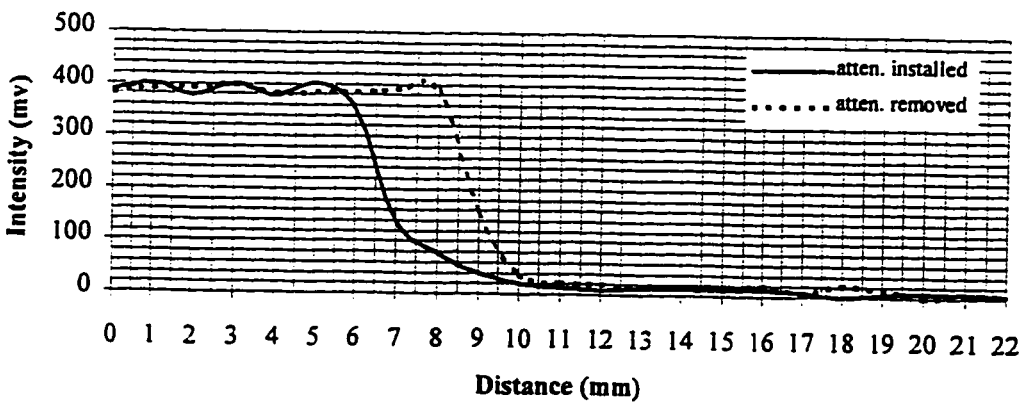

Fig. 5.2 : Intensity Variations (forward tilt , 5 °)

For the case where the sample is tilted with an angle of - 5°, the probe response is mostly constant up to a distance of 11 mm. After this region the intensity starts to drop rapidly for a distance of 5 mm after which it becomes insignificant. This is so because divergence of the beam takes place at a distance of 10 mm. Figure (5.3) shows this case, as can be observed from the curves that, the removal of the attenuater has no impact on the behavior of intensity. In reality, this case is expected to produce the same pattern as the one with a negative tilt however, because of the noise introduced into the system they appear different.

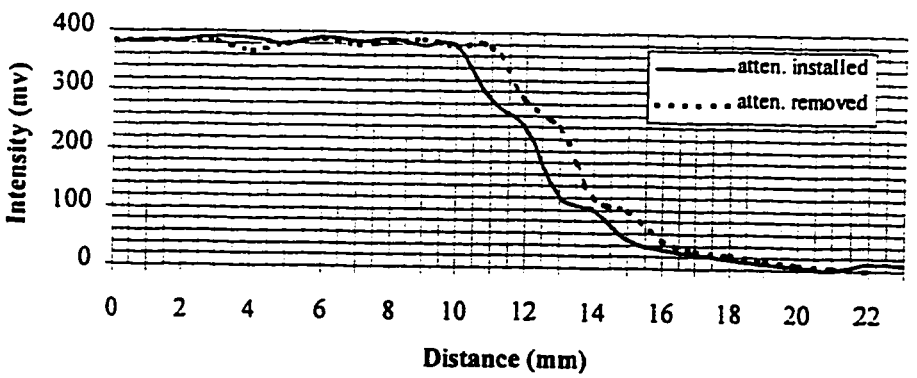

Fig. 5.3 : Intensity Variations (backward tilt , - 5 °)

The ratio (Io / I) has been plotted against the distance, for the parallel case (Figure 5.4) it can be seen that the probe response is almost constant up to a distance of 9 mm after that the ratio drops down to 0.55. At this value the probe response regained its constancy starting at a distance of 16 mm and continued till the end of the distance (x = 22) of measurement. The probe response is maximum when distance setting (initial probe position) is zero and the divergence occurs from the initial probe response resulting the values to drop suddenly (especially at x = 9 mm). The divergence reaches a constant value at a distance of 16 mm from the initial probe position so that, the intensity ratio remains unchanged at a value of 0.55.

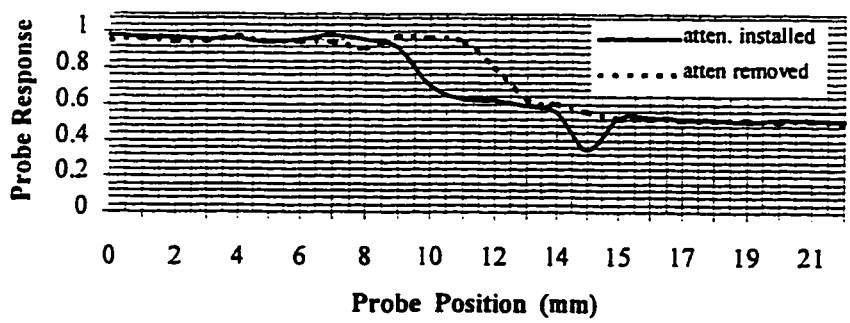

Fig. 5.4 : Probe Response (tilt angle = 0)

The sample is tilted with an angle of + 5 ° and the resulting ratio profile is plotted as shown in Figure (5.5). As can be seen from the plot that, the deviation of beam intensity occurs at a distance of 5 mm when the attenuater is installed. However, when the attenuater is removed this deviation occurs at a distance of 9 mm, this may be the effect of the attenuater or the beam intensity. However ratio remains constant after the distance of 10 mm all the way down to 22 mm. It is evident that, agreement between two curves is obvious which indicates that the attenuater has no effect on the profile at initial and final stages of the profile.

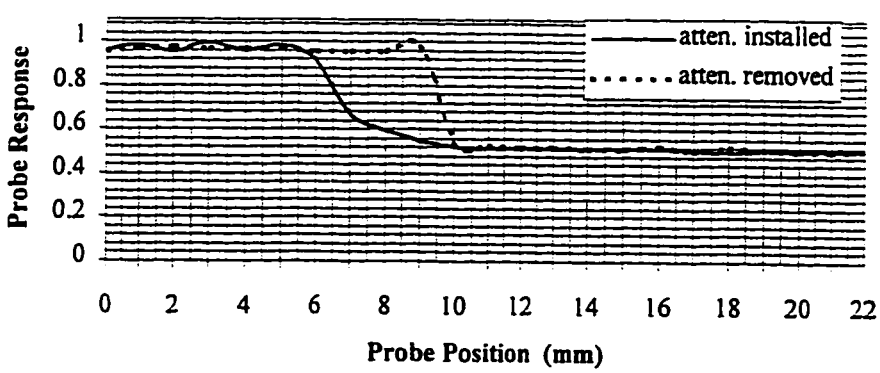

Fig. 5.5 : Probe Response (tilt angle = + 5°)

When comparing Figures (5.1 & 5.4), it is clear that the behavior of two curves are identical, therefore, the fluctuations in the incident laser beam intensity must be very minor, if that occurs so.

Finally, the sample is tilted backward with an angle of -5° and the resulting ratio profile is plotted as shown in Figure (5.6). There are some fluctuations at the beginning of the profile occur, but the substantial deviation of the beam intensity occurs at a distance of 12 mm after which the two curves dropped simultaneously. It can be seen that, the attenuater has no effect on the profile.

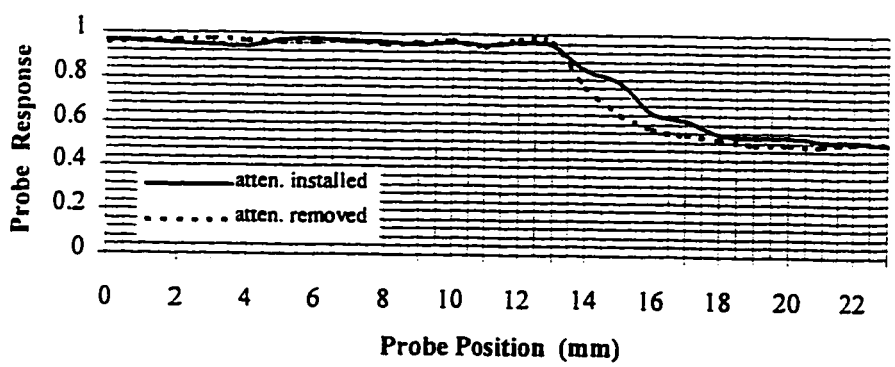

Fig. 5.6 : Probe Response (tilt angle = -5°)

Regular And Irregular Patterns

Figure (5.7) shows the photographs of sample surfaces. Scratches and irregular grinding are evident from the photographs. The patterns of this irregularity may be distinguished into two groups . In the first group, regular and horizontal scratches can be identified. However, in the second group, the patterns appear to be irregular due to horizontal and vertical scratches occurring in the grinding plane. Consequently, irregular patterns may be difficult to monitor by the stylus equipment, since the size of the scratches is only a couple of μm or less. On the other hand, these irregularities can possibly be detected by the optical probe, since the measurement relies on the reflection of light from the pattern. It should be noted that, when the size of the scratches reduces to $\lambda / 4$ (where λ is the wavelength of the incident light), the pattern can no longer be detected by any accuracy.

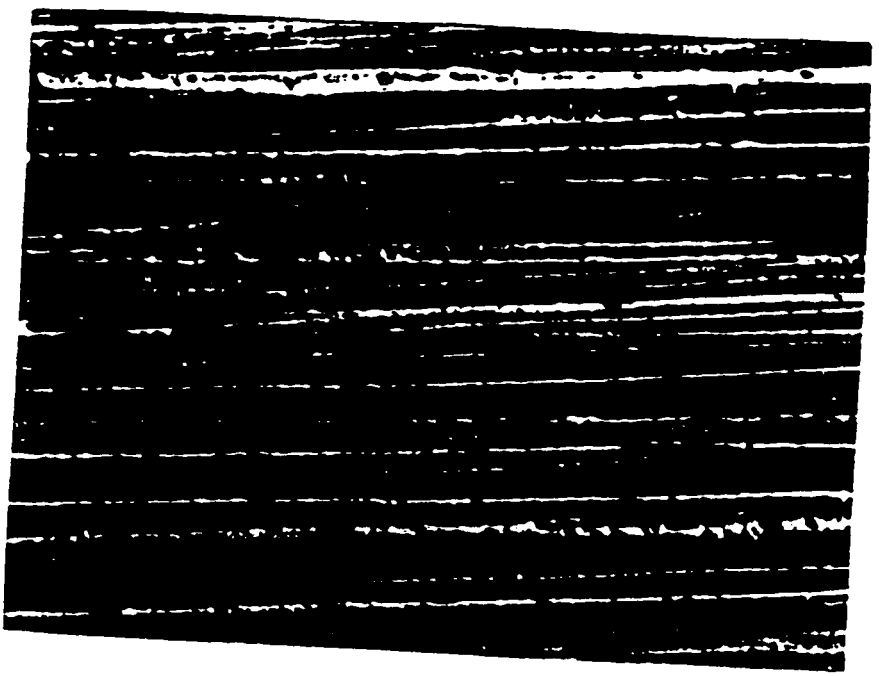

1 - Regular Pattern

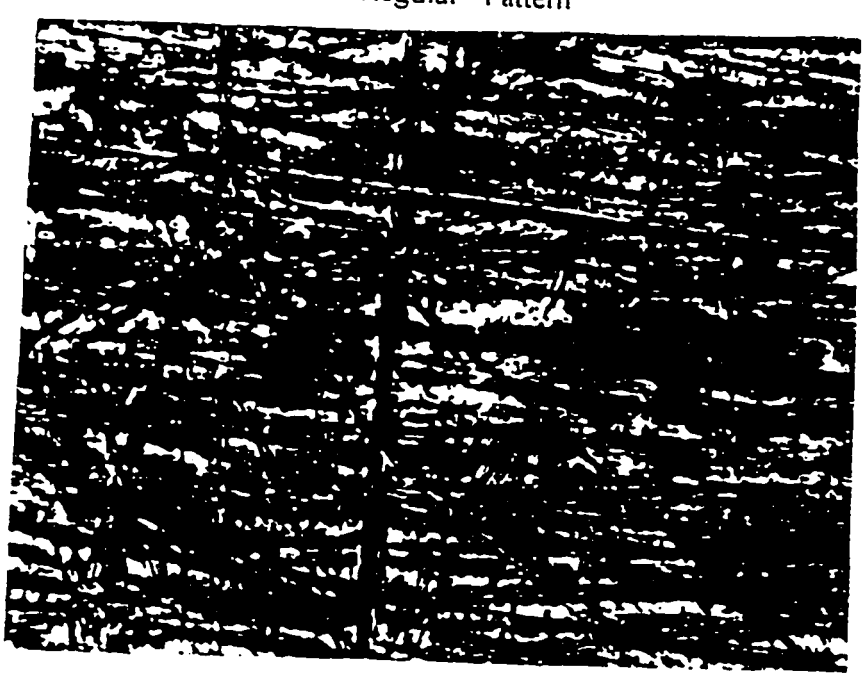

2 - Irregular Pattern

Fig. 5.7 : Photographs of different patterns .

3 - Irregular Pattern

Fig. 5.7 (Contd.) : Photographs of different patterns.

5 - 2 : OPTICAL SYSTEM OUTPUT RESULTS

The optical system generated 1025 data points of intensity ratios (Io / I). These data points were resulted when scanning a length of 15 mm on each sample. For each of the samples, every 20 readings are averaged and presented as one point on the graphs (as shown throughout this section) which constitutes a scanned length of 0.3 mm.

Knowing that , amplitude and spacing are the two basic independent features of the irregularities that make up the surface texture (in addition to mean line) and by looking to the profile of sample 1 which is shown in Figure (5.8) it can be seen that the profile displayed some fluctuations especially at x = 9 mm, the maximum peak to valley height (ratio) over the whole evaluation length is 0.0327: This value is directly affected by scratches or residual dirt on the surface. When considering the spacing of the peaks, it may be noted that, some local peaks, particularly those of small amplitude are not part of the surface and are not repeatable, being due to noise in the detection system, vibration, or residual dirt on the surface. This may be seen clearly in the profile of sample 1 at point 27 which corresponds to a scanned length of 8 mm. When looking carefully to the profile of sample 1 and compare it with the rest of profiles, one might observe that, the spacing between peaks is not consistent and non-uniform, this indicates that, sample 1 is relatively rough.

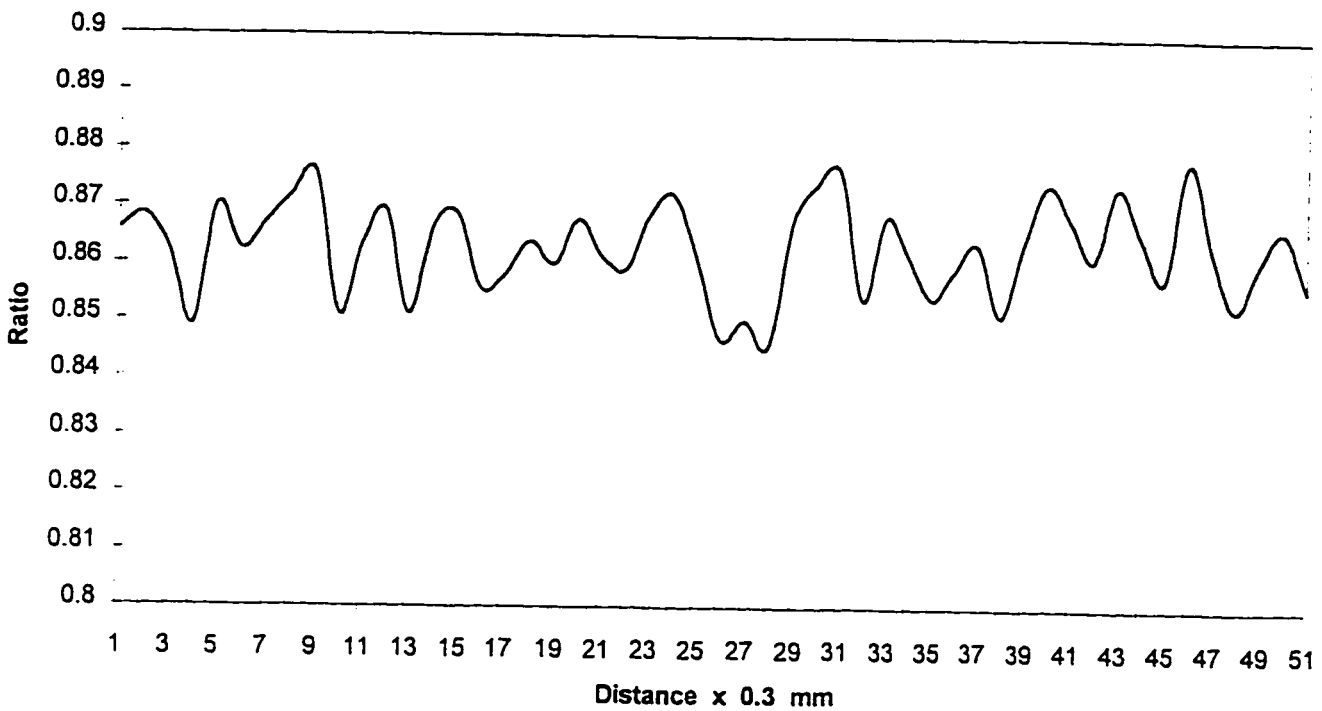

Fig. 5.8 : Intensity Variations For Sample No. 1

When using the optical method the mean line value of each profile has to be determined and considered among factors that contribute to surface texture. The mean value of oscillation for sample 1 is found to be 0.862823 which represents the ratio (intensity of reflected beam / intensity of reference beam), as this value is getting bigger the smoothness increases and vice versa.

Sample 2 had a maximum peak to valley value of 0.0386. When comparing this value to the value obtained for sample 1, it can be seen that, sample 2 (Figure 5.9) has more scratches than sample 1. this is of course affecting the surface roughness and hence the profile. Non uniformity is predominant over the surface of the sample since spacing between peaks is not in uniform harmony. The mean line value obtained for sample 2 is 0.834795 which is lower than that corresponds to sample 1.

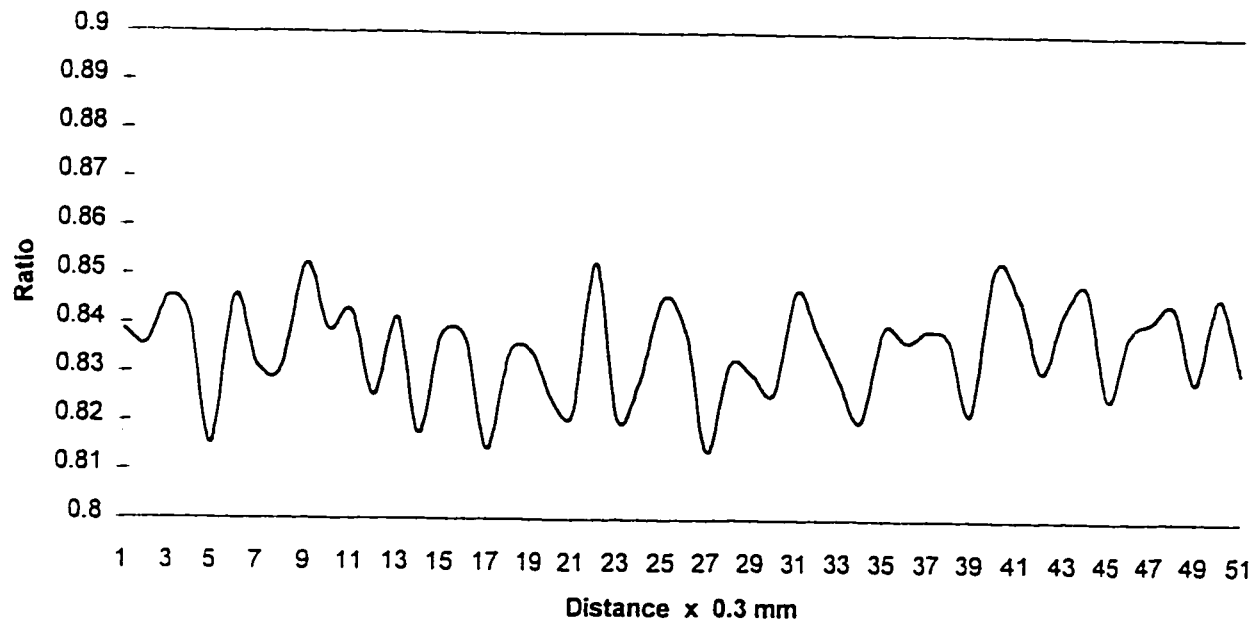

Fig. 5.9 : Intensity Variations For sample No. 2

Sample 3 has a maximum peak to valley value of 0.052 which is resulted form the overshooting occurred in the profile between points 10 and 12 that is shown in Figure (5.10). This abrupt change may happen because of the presence of uneven spot (< 0.6 mm in diameter) on the surface. The incident beam has been absorbed partially as it passed over this area and consequently the detector read the low value of the reflected beam intensity.

When calculating the mean value of oscillation, it reads 0.877661. The profile in this case is shifted up which indicates that, the detector read the highest intensity values compared to the rest of the profiles, therefore, sample 3 is the smoothest.

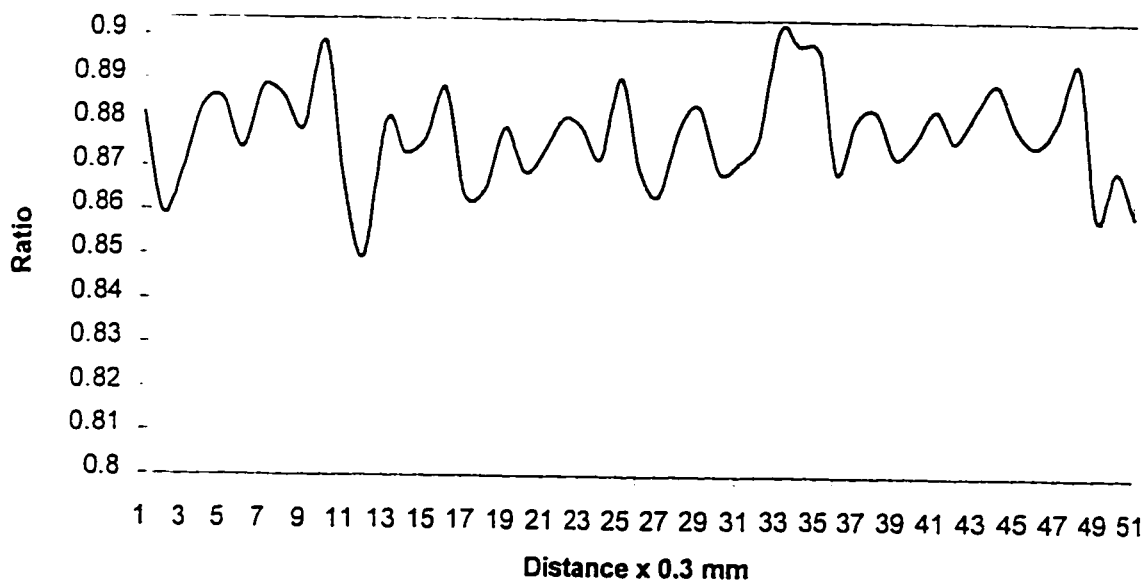

Fig. 5.10 : Intensity Variations for Sample No. 3

Samples 4 and 5 show similar profiles, the maximum peak to valley height for sample 4 is 0.0294 and it is 0.03588 for sample 5. Their mean values of oscillations obtained from stylus and optical measurements are close to each other (0.832 for sample 4 & 0.835 for sample 5). However, some deviation from both results is evident when considering sample 4. Their profiles are shown in Figs. 5.11 & 5.12.

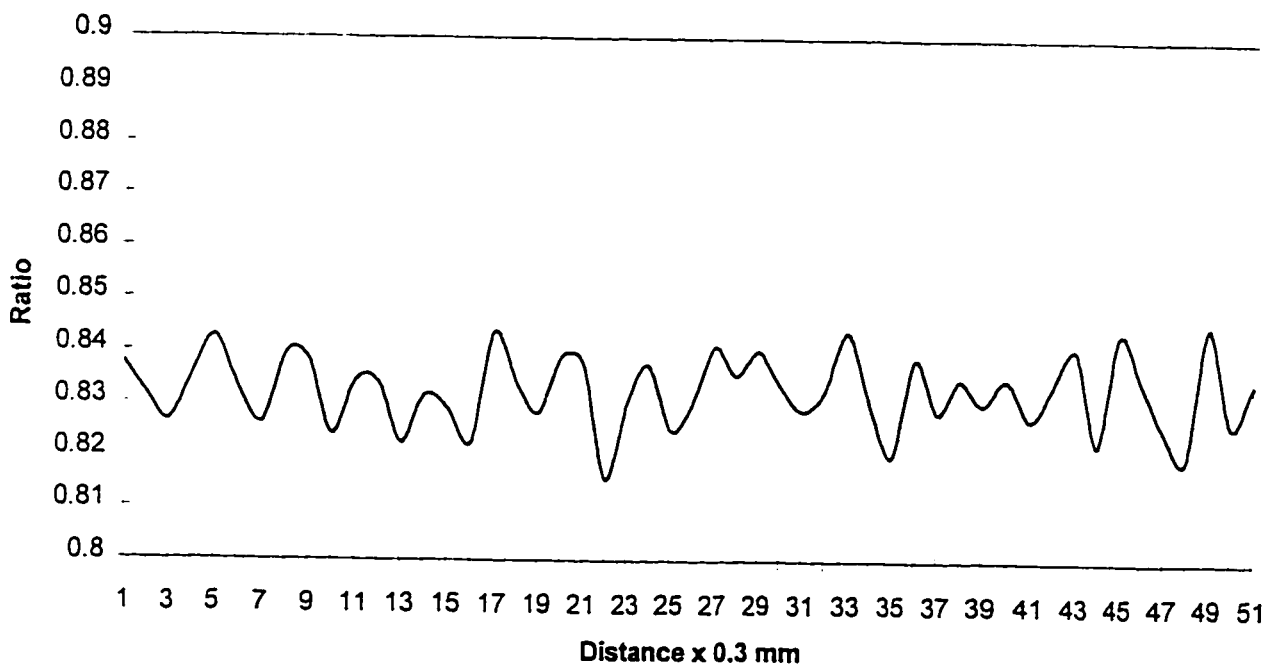

Fig. 5.11 : Intensity Variations For Sample No. 4

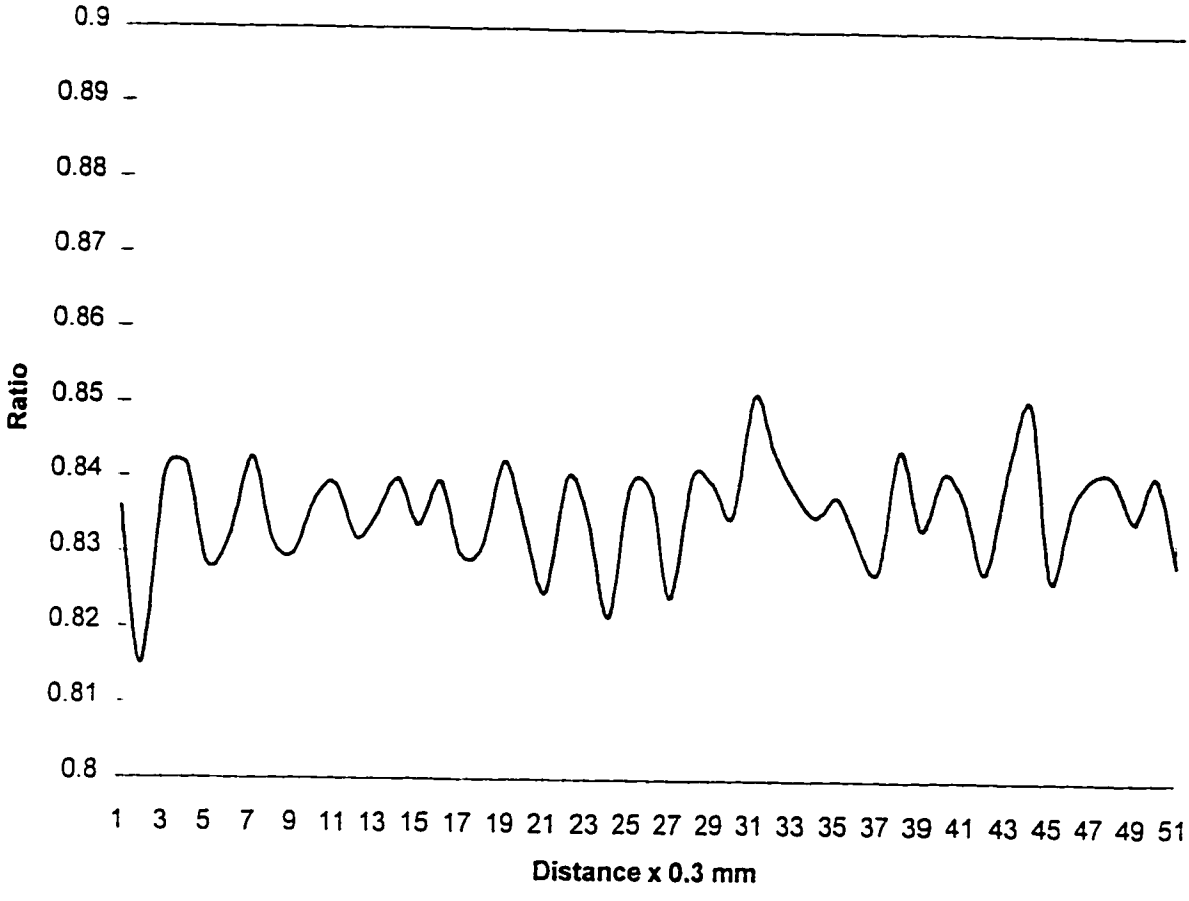

Fig. 5.12 : Intensity Variations For Sample No. 5

The average roughness values obtained by using the optical method are plotted for all workpiec surfaces as shown in Figure (5.13). By looking at the Figure 5.13, it can be seen that, surface type 1 is the roughest while surface 3 is the smoothest compared to other surface types.

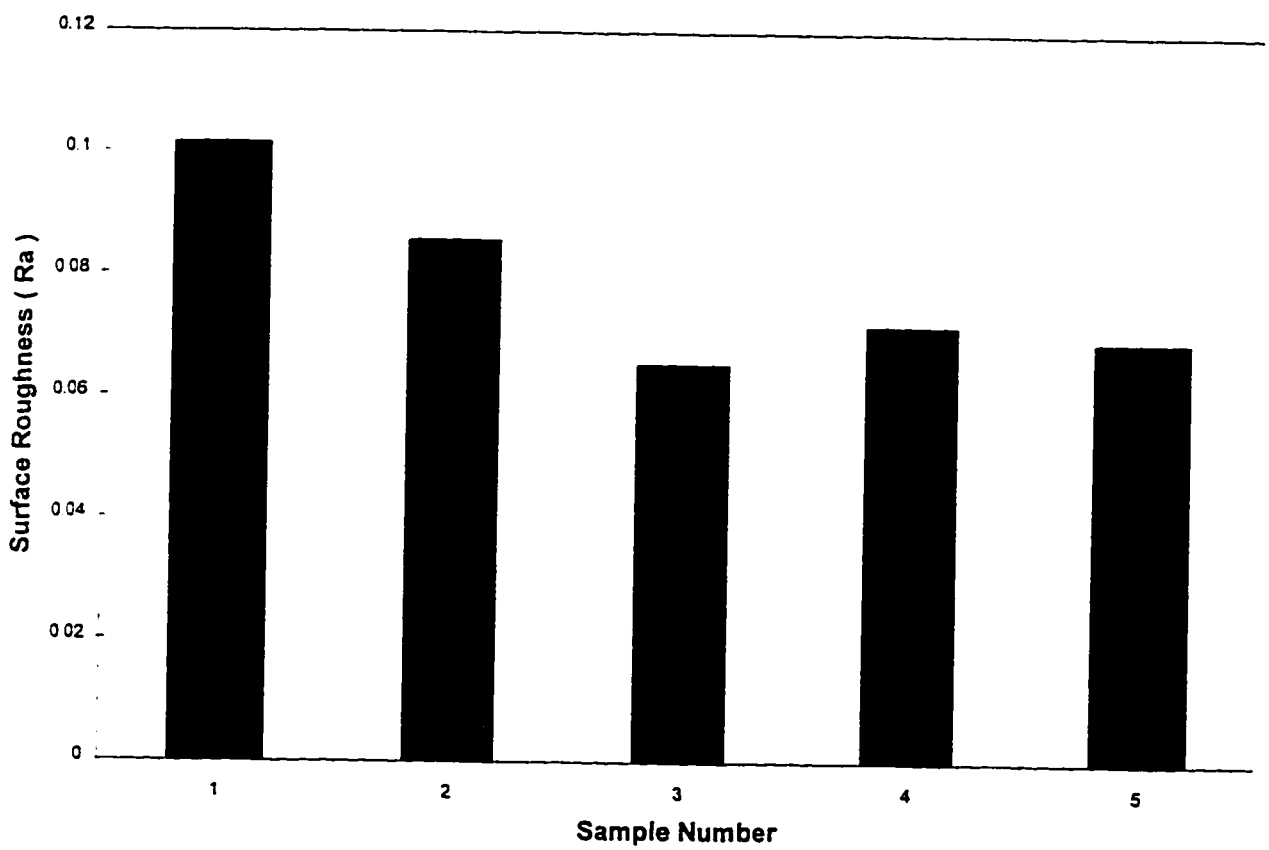

Fig. 5.13 : Surface Roughness Values Obtained From Optical Method For All Tested Surfaces.

5 - 3 : NEURAL NETWORK RESULTS

The four control chart patterns are considered, these include normal pattern, cyclic, increasing trend and decreasing trend as shown in Figure 5.14. It is possible to produce a series of the numbers resembling the specific patterns. 2200 patterns and their desired outputs are generated. 1800 of them are used to train the network and the remaining patterns are kept for testing the network performance. Mathematics for generating the control chart patterns is given below :

(1) Normal Patterns :

$$y(t) = \mu + r(t) \times \sigma \qquad (5-1)$$

(2) Cyclic Patterns :

$$y(t) = \mu + r(t) \times \sigma + a \times \mathrm{Sin}(2 \times \pi \times t / T) \qquad (5-2)$$

(3) Increasing and Decreasing Trends :

$$y(t) = \mu + r(t) \times \sigma \pm g t \qquad (5-3)$$

where :

μ : Mean value of the process variable being monitored (taken as 90).

σ : Standard deviation of the process (taken as 6).

a : Amplitude of cyclic variation (taken as 55 or less).

g : Magnitude of the gradient of the trend (taken as being in the range 0.2 to 0.5).

r : Normally distributed random number (between -3 and +3).

t : Discrete time at which the pattern is sampled (taken as being within the range 0 to 99).

T : Period of a cycle (taken as being in the range 4 to 16 sampling intervals).

$y(t)$: Sample value at time t.

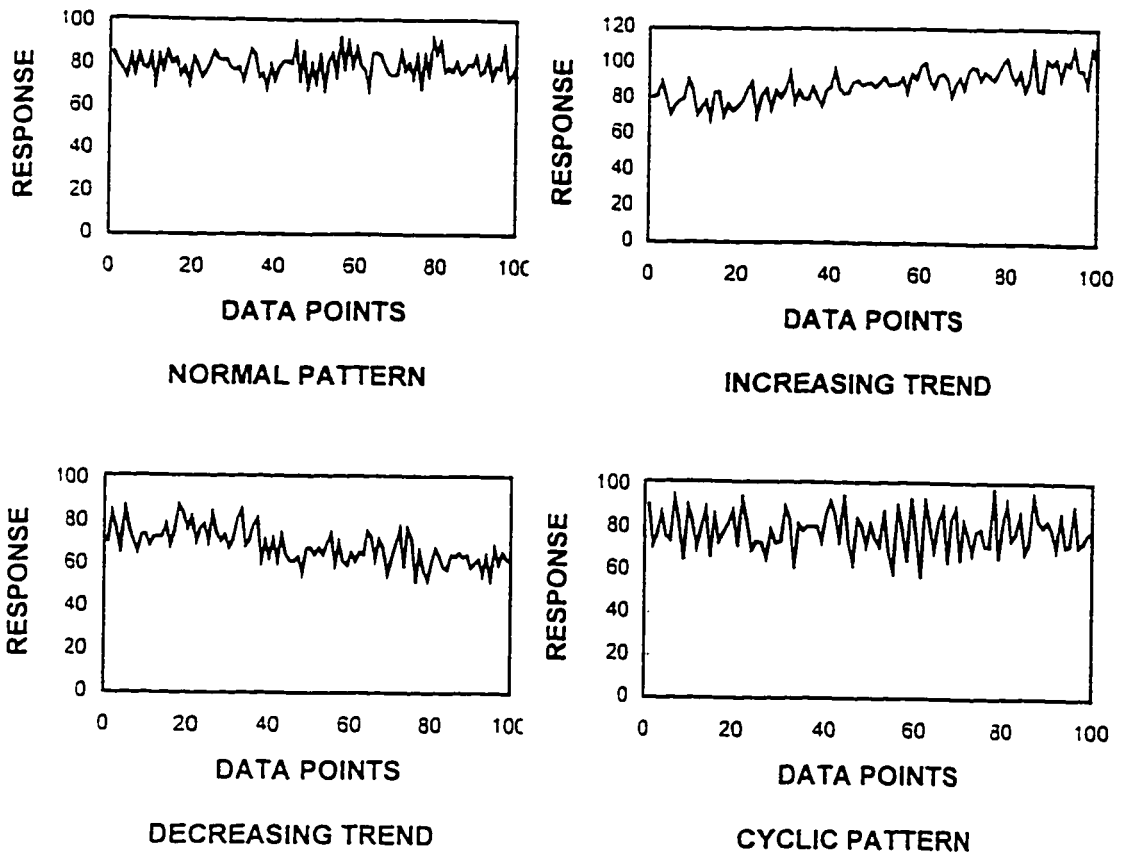

Fig. 5 - 14 : Train And Test Patterns Developed Mathematically

When testing the actual surface profiles, the neural network classified the patterns with high performance providing that the network confused the patterns 1, 2 and 4 (Fig. 5.15). In this case, the resulting surface profile for the workpieces 1, 2 and 3 may appear similar to the normal, cycle, as well as the decreasing trend. However, the surface profiles show more towards to the normal pattern, since the network performance for normal pattern is higher than those correspond to other patterns. On the other hand, the performance of the network is higher towards to the cyclic pattern when testing the surface profiles of workpieces 4 and 5. Consequently, surface profiles corresponding to different workpiece differ in appearance and this may be easily classified by the network developed.

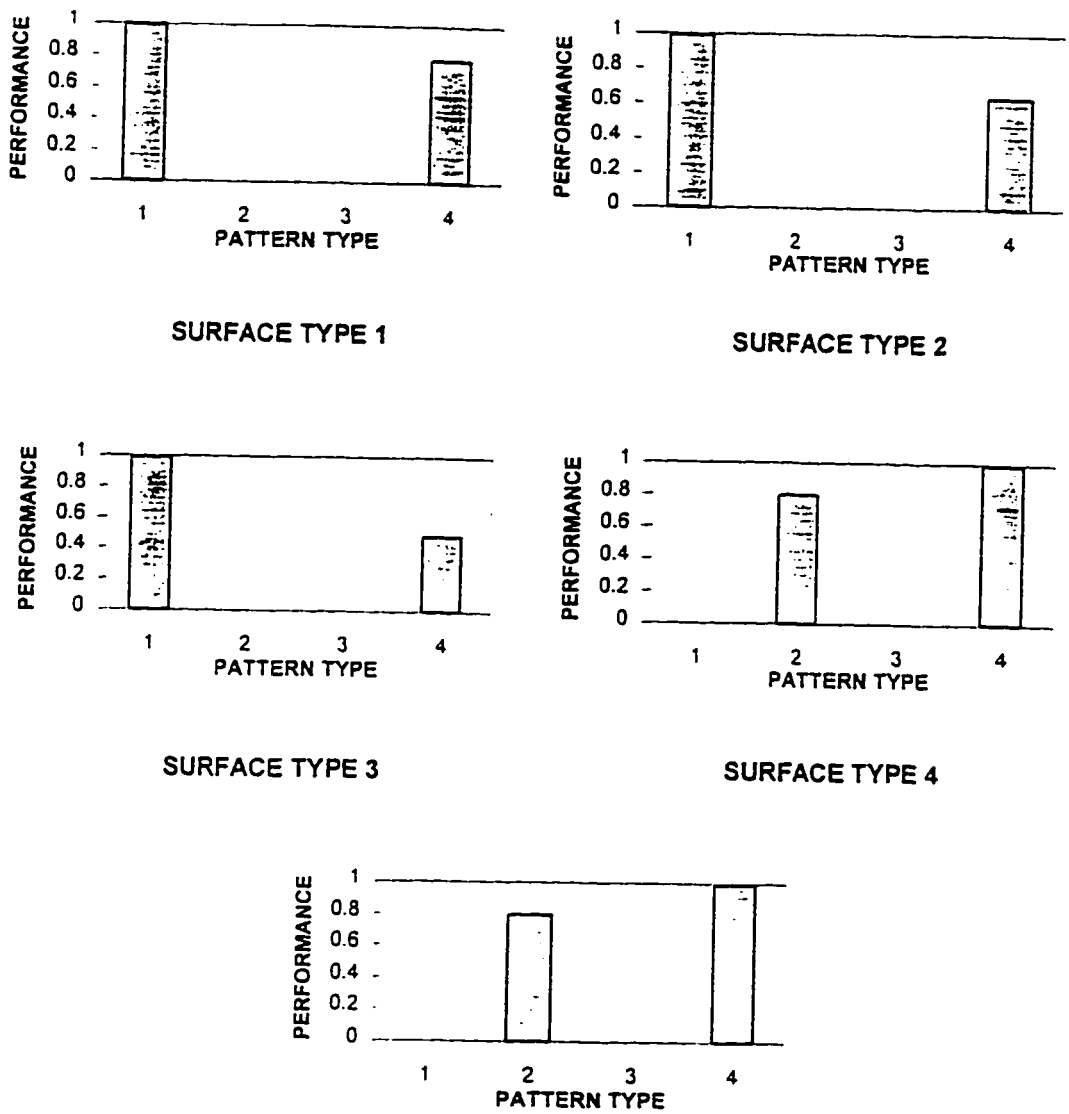

Fig. 5.15 : Neural Network Output For All Workpiece Surfaces .

5.4 -COMPARISON OF OPTICAL AND MECHANICAL MEASUREMENT METHODS :

Figure (5.16) shows the profile obtained by the stylus instrument (Linear Profiling System) when testing surface type 1. The horizontal and vertical scales are shown on the figure noting that. the rest of the surfaces are measured by the same instrument and scale.

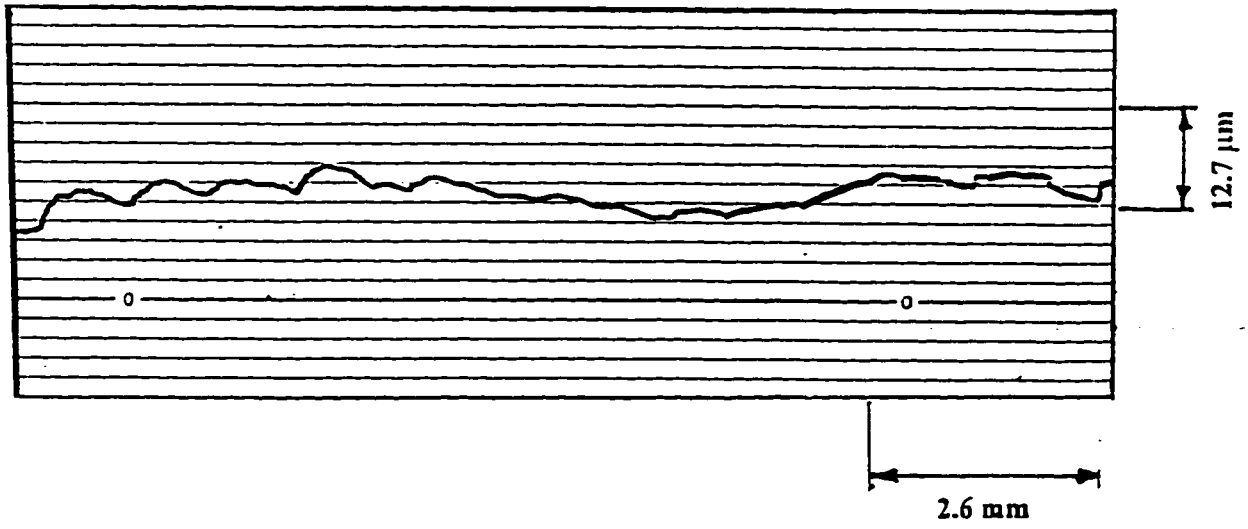

Fig. 5.16 : Stylus measurement result for surface type 1.

Mechanical and optical measurements are performed for all workpiece surfaces, and the resulting figures are tabulated in Table (5.1) which gives the surface roughness (Ra) values. Ra attains the same trend for both measurements. It should be noted that, Ra values measured by both methods have been normalized based on the maximum value. By looking to the table, it can be seen clearly that, the qualitative agreement in both results is evident.

Table 5.1 : Ra values obtained from both optical and mechanical measurements for different workpiece surfaces.

Surface Type	1	2	3	4	5
Optical Measurement Ra	1	0.843	0.643	0.705	0.681
Mechanical Measurement Ra	1	0.815	0.656	0.742	0.743

5.5 - FUTURE WORK :

The present optical system is able to provide information about the surface roughness of the workpiece in one-dimension. This is due to the movement of the workpiece, which is one-dimensional motion. However, this design can be improved and make the workpiece movement into two and / or three dimension. In this case, the surface topology may be recorded with sufficient accuracy. In addition to this, the accuracy of the mechanism may be improved when installing a feed back system in controlling the sample holder motion.

On the other hand, specular reflection of the surface may be included when setting the probe at low angles reference workpiece surface. In this case, a mathematical model may be introduced to predict the possible reflection patterns, which then be compared with the measurement results.

The neural network used in the present system employs 100 neurons in the input layer. This may be expanded to more neurons, in order to obtain better accuracy when classifying the resulting surface profiles.

CHAPTER 6

CONCLUSIONS AND RECOMMENDATIONS

The conclusions and recommendations derived from the present work may be listed as follows :

1 - The probe position relative to the workpiece surface becomes critical as the distance between the probe and the workpiece increases. However, beam attenuater installed in the path of incident laser beam does not have a significant effect on the probe response providing that attenuation of the order of 8 % occurs.

2 - Tilting of the workpiece surface affects the probe response such that early decay of probe response occurs when the distance between the probe and the workpiece surface increases.

3 - Optical method results agree well with the stylus measurement results qualitatively noting that the spatial resolution of the data obtained form the optical method is considerably high. Both tests classify surface 1 as the roughest and surface 3 as the smoothest relative to other used surfaces.

4 - Optical measurement is easier and considerably faster than the measurement done using the stylus machine. From an economical point of view, optical method is the preferred choice.

5 - Optical measurements have to be done in a clean environment, since dust can have a negative effect on the performance. Care should be taken to prevent any disturbance of light or interference during measurement, since optical measurement depends solely on light intensity.

6 - The backpropagation network classifies the surface profiles, in accordance with the patterns developed mathematically, with considerably high performance. Some surfaces show mix patterns, this mix is due to the instability and non-uniformity of the process applied on these surfaces, however, normal pattern is the dominant pattern which is evident from the network output. All surfaces exhibit to some degree the behavior of cyclic pattern (pattern 4) especially, surfaces 4 and 5 which are identical with regard to their average roughness. Surfaces 1, 2 and 3 do not have the characteristic of increasing and decreasing trends (patterns 2 and 3). It should be noted that, non of the surfaces exhibits decreasing trend (pattern 3).

7 - Laser light traces the surface profile more precisely than the stylus tip and overcomes the limitation of tip size. In addition to this, it leaves no marks and scratches on the surface being tested. Consequently, information collected about the surface profile using laser scanning technique enable investigators to get very close picture about the surface profile.

APPENDIX

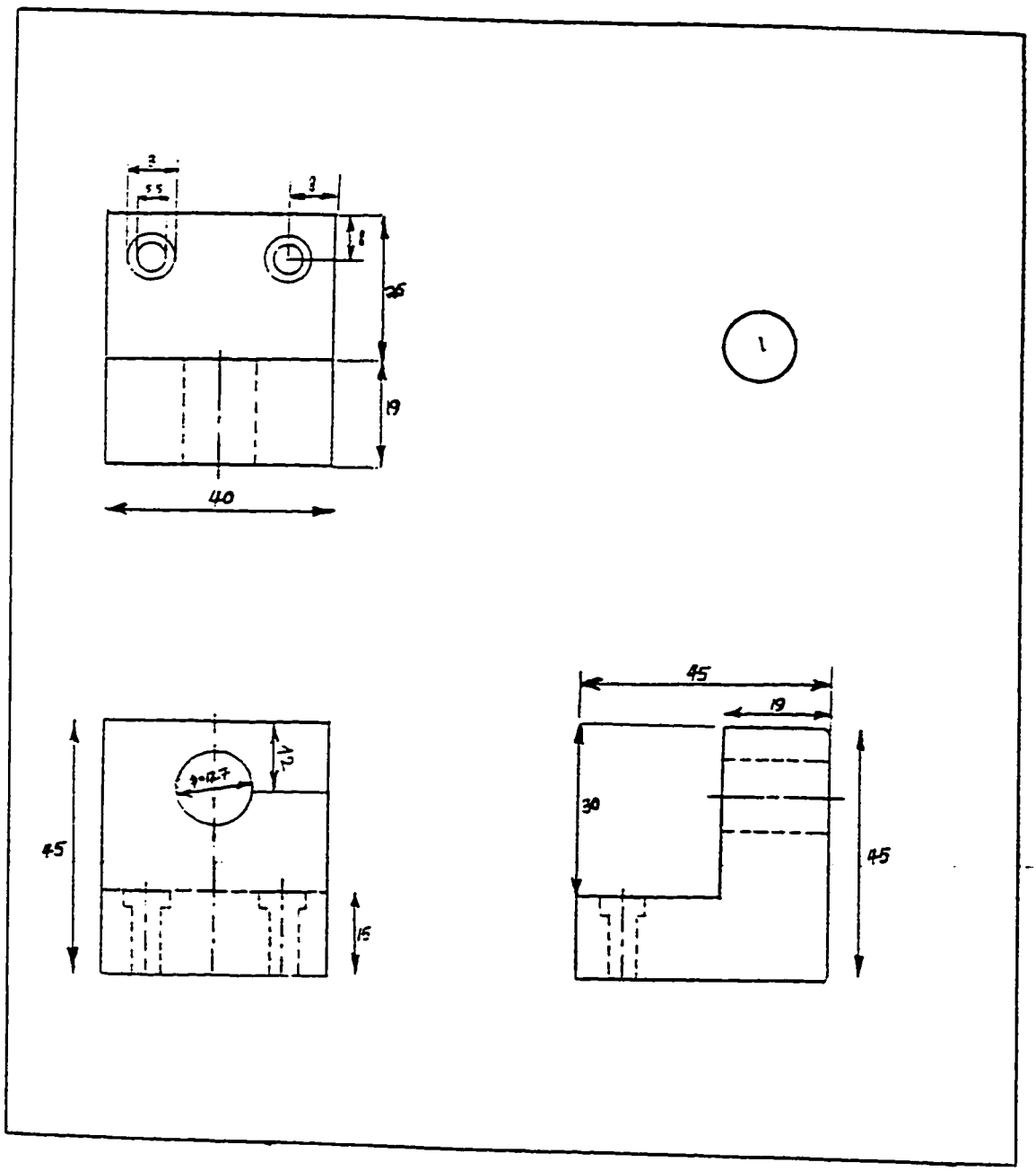

Fig. A.1 : Reference Probe & Laser Holder

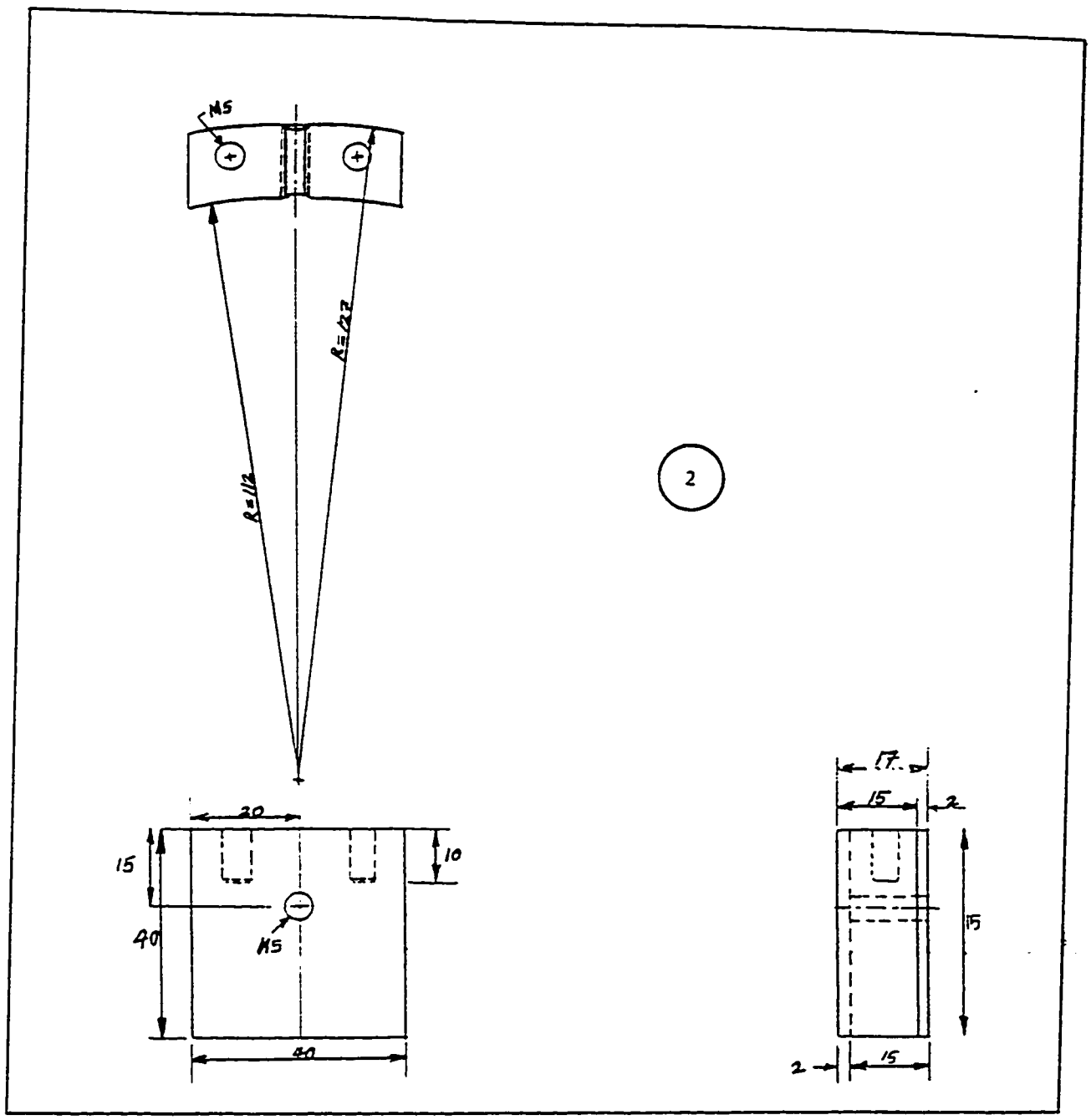

Fig. A.2 : Attached Arc (movable)

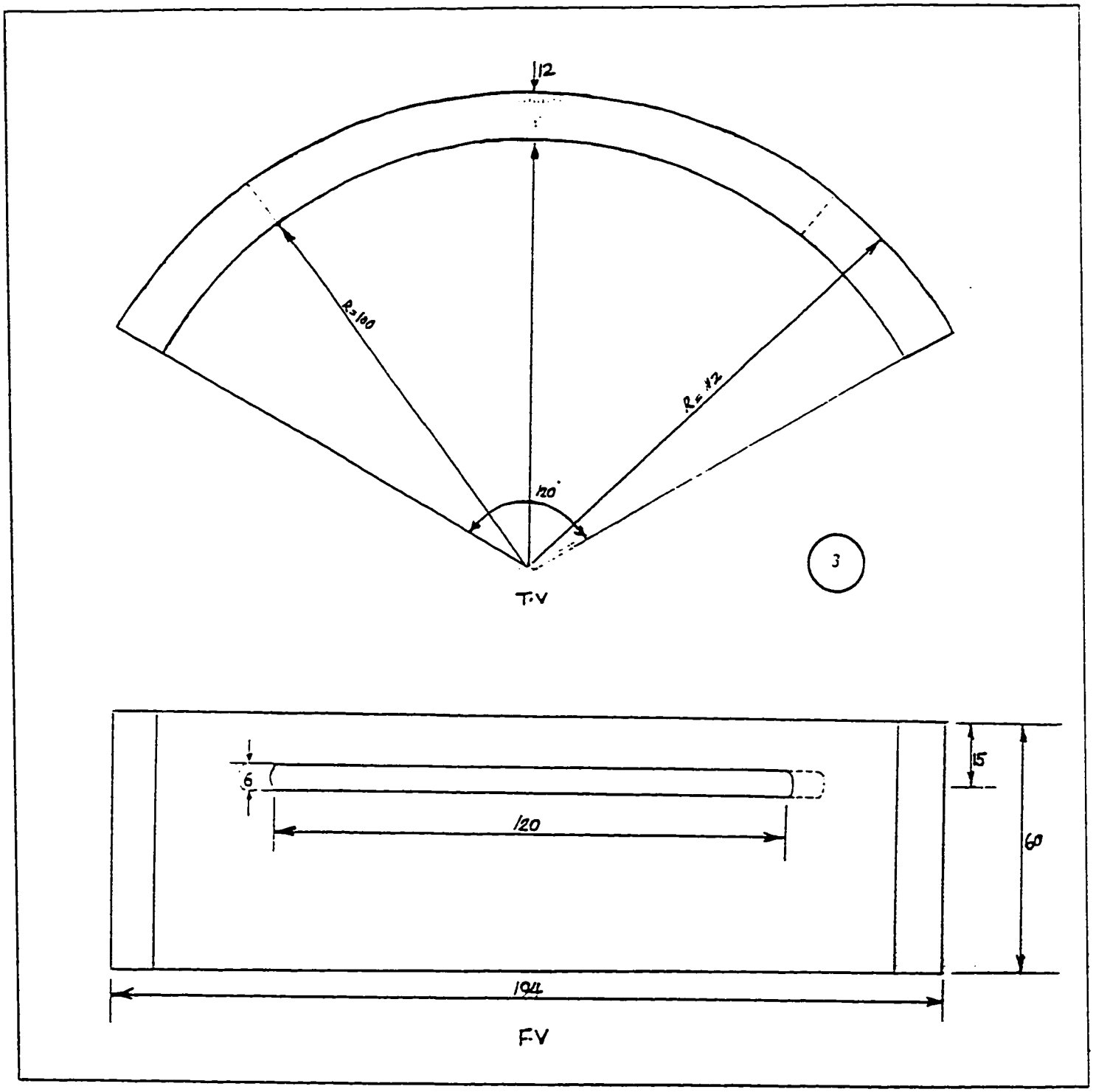

Fig. A.3 : Main Arc (stationary)

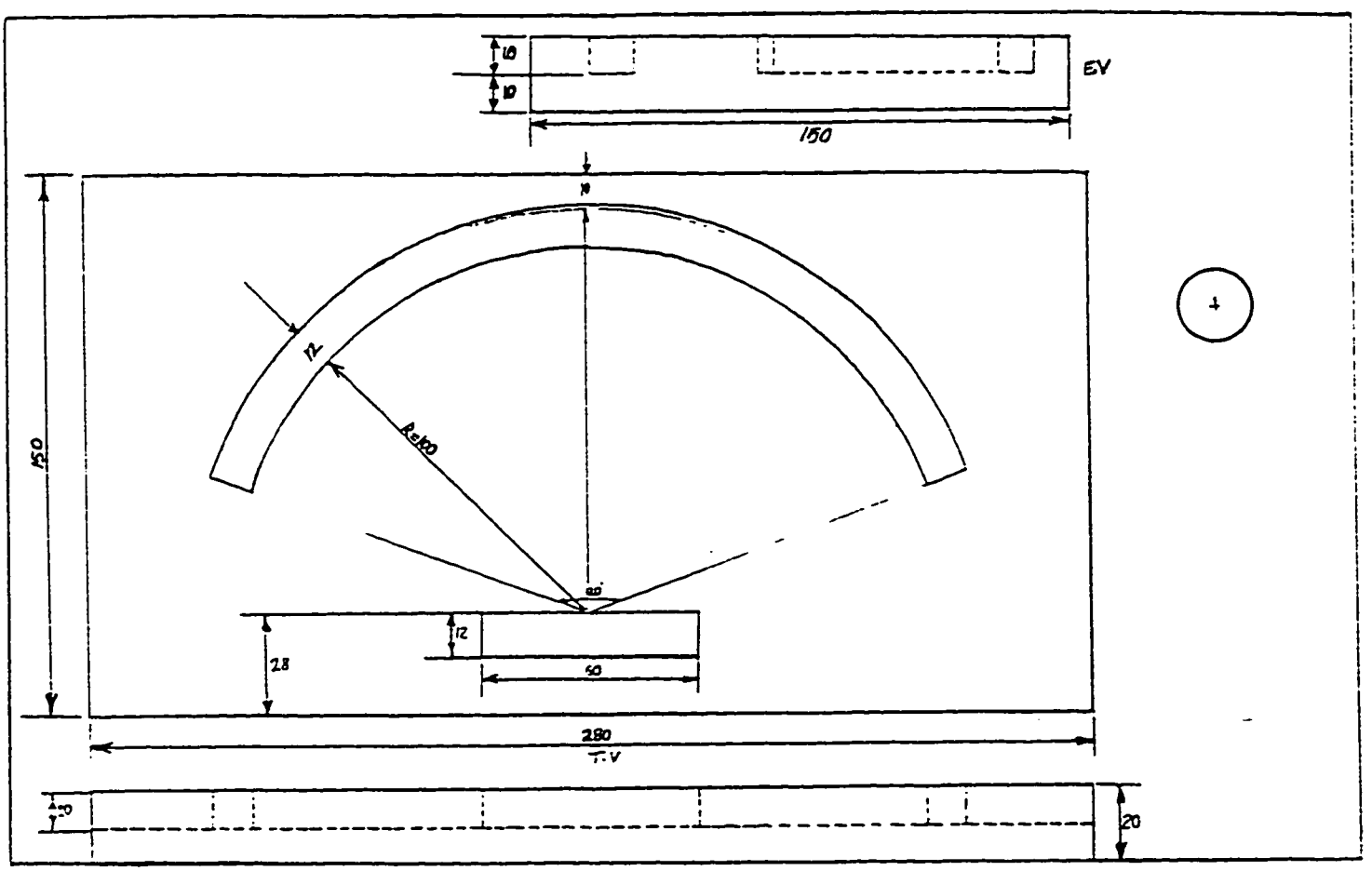

Fig. A.4 : Main Plate

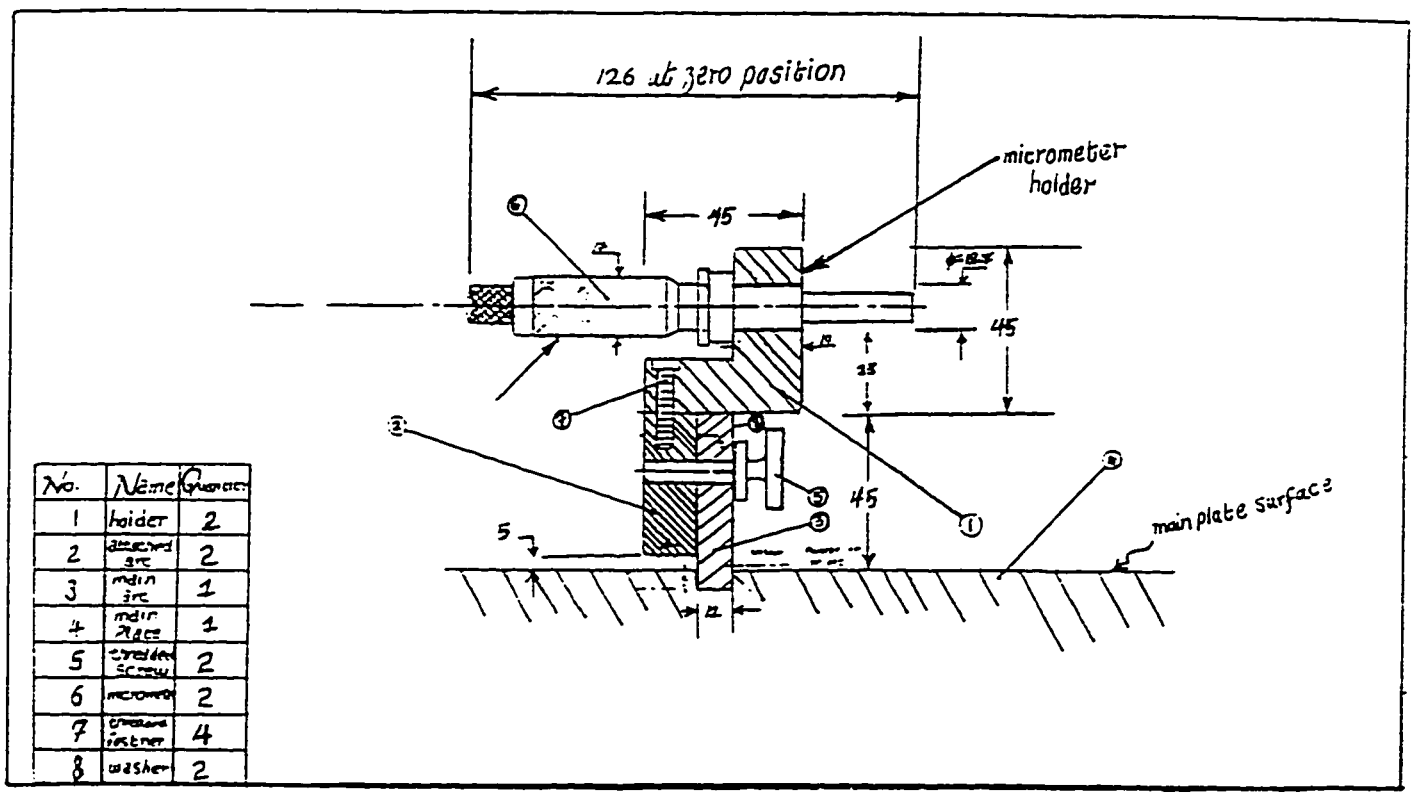

No.	Name	Quantity
1	holder	2
2	[illegible]	2
3	[illegible]	1
4	[illegible]	1
5	[illegible]	2
6	[illegible]	2
7	[illegible]	4
8	washer	2

Fig. A.5 : Cross Sectional View of The Micrometer

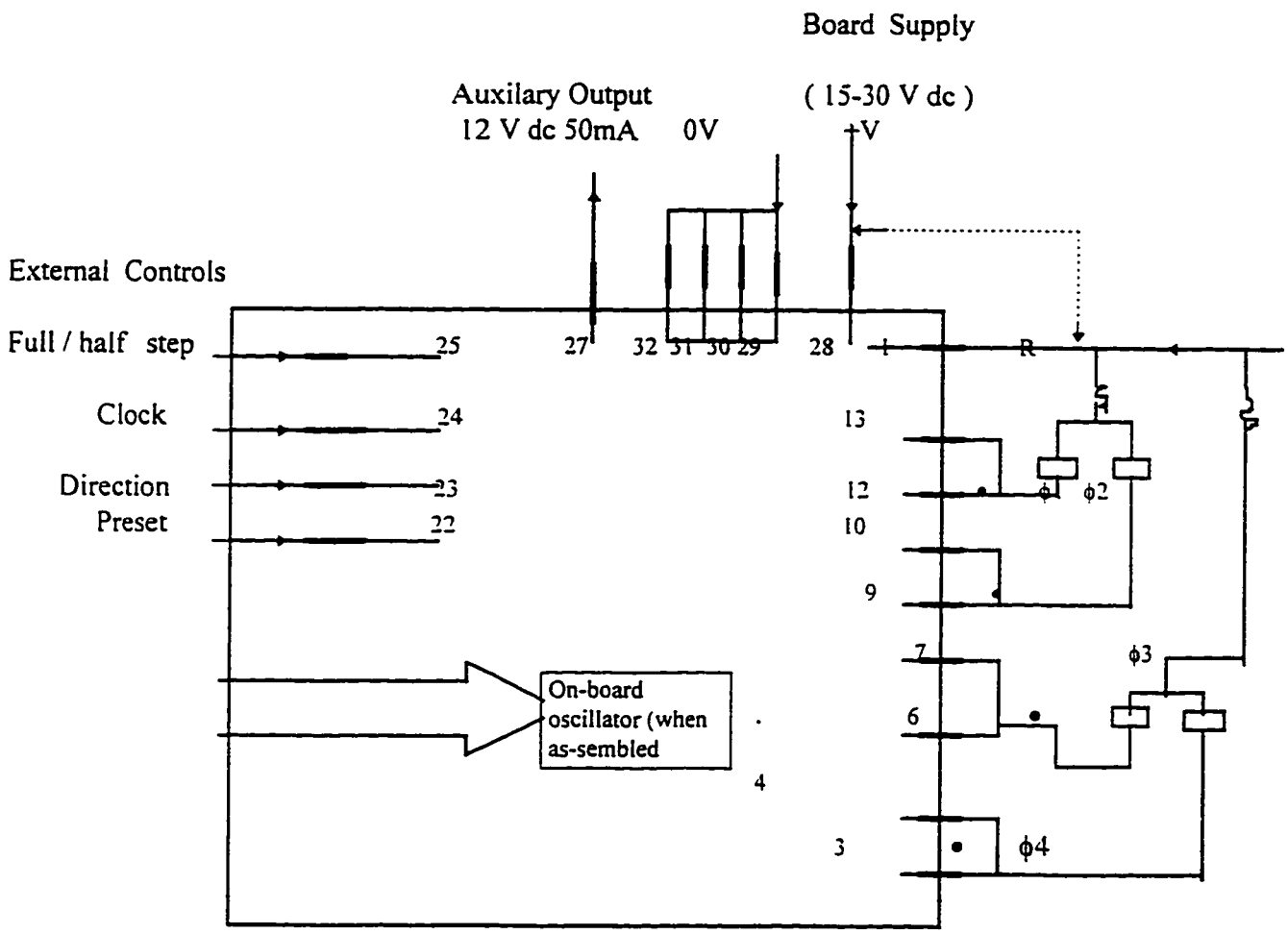

$$R = \frac{+V \text{ motor} - \text{rated winding voltage}}{\text{rated winding current}}$$

Fig. A.6 : Unipolar Stepper Motor Drive Board Connections

REFERENCES

[1] Bengtsson, A, " On three-dimensional measurement of surface roughness", Chalmers Tekniska Hogskola, Doktorsavhandlinger, no.809, 1991. Publ. By Chalners Tekniska hogskola, Gotenberg, Sweeden.

[2] B. Ramamoorthy and V. Radhakrishnan. , " Statistical approaches to surface texture classification " , pp. 155 - 161, 1993.

[3] Brenner Dean ; Principe, Jose C. ; Doty , Keith L. , " Neural network classification of metal surface properties using a dynamic touch sensor " , pp. 189-194 , July 1991.

[4] Dayhoff J. E ., " Neural Network Architectures : an introduction ", Van Nostrand Reinhold,

New York , 1 st Ed., pp . 58 - 78, 1990.

[5] Domanski, A.W.,and Wolinski, T.R., " Surface roughness measurement with optical fibers ", IEEE Transactions on Instrumentation and measurement , vol.41, no.6, pp.1057-1061, Dec.1992.

[6] F. G. Parsons and A. N. Tabenkin , " The theory and development of user-friendly software for the measurement of surface roughness and geometrical parameters ", Vol. 32, No. ½ , pp. 255 - 262 , 1992.

[7] Galente, G.,Piacentini, M. and Ruisi , V. F., " surface roughness detection by tool image processing " , Wear , vol.148,no.2, p. 211,Aug. 1991.

[8] G. Rzevski and R. A. Adey , " Application of Artificial Intelligence in Engineering VI ",

pp. 423 - 433 , 1991.

[9] Hinton G.," Connections Learning Procedures ", Artificial Intelligence , Vol.40 , pp.185 - 234 , 1989.

[10] Huang, Samuel H. ; Zhang, Hong-Chao , " Artificial neural networks in manufacturing : concepts, applications, and perspectives", V. 17 , pp. 212 - 228 , Jun 1994.

[11] J. D . Garratt & D . J . Nettleton , " A stylus Instrument for Roughness and Profile Measurement of Ultra-Fine Surfaces " , Vol. 32 , No. ½ , pp. 233 - 238 , 1992.

[12] Kurita , M., Sato,M., Sato, M. and Nakano,k.," Technique for rapidly measuring surface roughness using laser " , JSME Int. J., Series 1 ; Solid Mechanics , Strength of materials , vol.35, no.3, pp. 335-339, July 1992.

[13] Lin, Psang Dian ; Chen, Yu Lung , " Laser surface height and orientation measurement system " , ASME V. 116 , pp. 265-271 , June 1994.

[14] Matsumura, Takashi ; Obikawa, Toshiyuki; Shirakashi, Takahiro; Usui, Eiji, " On the development of expert system for selecting the optimum cutting conditions ", V 57, pp. 1053 - 1059 , June 1991.

[15] N. K. Myshkin, A. Ya Grigoriev and O. V. Kholodilov , " Quantitative analysis of surface topography using scanning electron microscopy " , pp. 119 - 133 . 1992.

[16] Payne, R.D., Matteson. M.A, and Moran A.L., " Application of neural networks in spray forming technology " . Int. J. of Powder Metallurgy ,vol 29, no.4, pp. 345-351, Oct. 1993.

[17] P. H. Osana and P. Totewa , " Workpiece accuracy - the critical path to economical production " , Vol. 32 , No. ½ , pp. 45 - 49 , 1992.

[18] R 468 " Surface roughness " , International Standards , 1960.

[19] Rank Taylor Hobson ," Exploring Surface Texture" , Leicester, England, List No. 600-7, pp. 5 - 125 , 1980.

[20] R. S. Components ," Product Catalogue " , R.S . Component Ltd ., P.O.Box 253, Birmingham B8 IBQ, UK.

[21] Rumelhart D.E., Richard D., Richard G., and Chauvin Y., " Backpropagation : Theoretical foundations " , Edited from Backpropagation and Theory , I st Ed., Lawrence Erlbaum,1992.

[22] Rumelhart R.D. and Mc.Clelland J., " Parallel distributed processing " , I st Ed., MIT Cambridge Press, 1986.

[23] Sathyanarayanan . G. ; Ilhan, R. E. ; Storer , R . H. ; Phillips , R. E. , " Study of wheel wear in electrochemical surface grinding " , V 114 , pp. 82 - 93 , Feb. 1992.

[24] Shukla, R.P.,Perera, G. M., Venkateswarlu, P. and George,M.C., " Interferometric techniques for correction of sample tilt in the sommergeon profilometer for surface roughness studies ", Optics and Laser Technology , vol.23,no.2,pp. 98-104-1991.

[25] Silvennoinen, R., Perponen,K.E., Askura, T., Zhang , Y.F., Gu, L.,ikonen , K.,and Moreley , F.J., "Specular reflectance of cold-rolled aluminum surfaces " , Optics and Lasre in Engineering ,vol.17, no. 2, pp. 103-109, 1992.

[26] Society of Manufacturing Engineers. " Manufacturing Engineering ", Vol. 115 No. 4 , p. 57. October 1995.

[27] T. Klimezak , " Origins , magnitude and statistical significance of differences between roughness parameters of two- and three-dimensional characteristics " , pp. 19 - 31 , 1992.

[28] Yilbas , B. S., Danisman , k., Yilmaz , M., and Yilbas , Z., " The development of the computer controlled electro-fiber system for surface roughness measurements" , SPIE vol. 776, Metrology of Optoelectronic System . pp. 55-58 , 1987.